HHS Public Access

Author manuscript

Nat Med. Author manuscript; available in PMC 2022 May 01.

Published in final edited form as:

Nat Med. 2021 November ; 27(11): 2002–2011. doi:10.1038/s41591-021-01542-z.

Immune Responses to Two and Three Doses of the BNT162b2 mRNA Vaccine in Adults with Solid Tumors

Rachna T. Shroff[1], **Pavani Chalasani**[1], **Ran Wei**[2], **Daniel Pennington**[1], **Grace Quirk**[3], **Marta V. Schoenle**[2,3], **Kameron L. Peyton**[2], **Jennifer L. Uhrlaub**[2], **Tyler J. Ripperger**[2], **Mladen Jergović**[2], **Shelby Dalgai**[1], **Alexander Wolf**[1], **Rebecca Whitmer**[8], **Hytham Hammad**[1], **Amy Carrier**[1], **Aaron J. Scott**[1], **Janko Nikolich-Žugich**[2,3,6], **Michael Worobey**[3,4], **Ryan Sprissler**[3,5], **Michael Dake**[7], **Bonnie J. LaFleur**[3], **Deepta Bhattacharya**[2,3]

[1]Division of Hematology and Oncology, Department of Medicine, University of Arizona Cancer Center, Tucson, AZ, USA.

[2]Department of Immunobiology, University of Arizona College of Medicine, Tucson, AZ, USA

[3]BIO5 Institute, University of Arizona, Tucson, AZ, USA

[4]Department of Ecology and Evolutionary Biology, University of Arizona, Tucson, AZ, USA.

[5]University of Arizona Genomics Core and the Arizona Research Labs, University of Arizona Genetics Core, University of Arizona, Tucson, AZ, USA

[6]University of Arizona Center on Aging, University of Arizona College of Medicine, Tucson, AZ, USA

[7]Office of the Senior Vice-President for Health Sciences, University of Arizona, Tucson, AZ, USA

[8]The University of Arizona College of Medicine, Tucson, AZ

Abstract

Vaccines against SARS-CoV-2 have shown high efficacy, but immunocompromised participants were excluded from controlled clinical trials. We compared immune responses to the BNT162b2 mRNA COVID-19 vaccine in patients with solid tumors (n=53) on active cytotoxic anti-cancer therapy to a control cohort without cancer (n=50). Neutralizing antibodies were detected in 67% of cancer patients after the first immunization, followed by a 3-fold increase in median titers after the second dose. Similar patterns were observed for Spike protein-specific serum antibodies and T cells, but the magnitude of each of these responses was diminished relative to the control cohort. In most cancer patients, we detected Spike receptor binding domain- and other S1-specific memory B cell subsets as potential predictors of anamnestic responses to additional immunizations. We therefore initiated a phase 1 trial for 20 cancer cohort participants of a

Corresponding authors: Rachna T. Shroff (rshroff@arizona.edu), Bonnie LaFleur (blafleur@arizona.edu) and Deepta Bhattacharya (deeptab@arizona.edu).

Authors' Contributions:

Concept, Clinical Protocol Development: RTS, PC, DP, MD, BJL, DB

Experimental Design and Data Analysis: RW, GQ, MS, KP, TJR, JLU, MJ, MW, RS, JNZ, BJL, DB

Accrual of patients, data entry, AE collection: RTS, PC, DP, SD, AW, HH, AJS, AC, RW

Competing interests:

The remaining authors declare no competing interests and no authors are employees of relevant companies.

third vaccine dose of BNT162b2 (NCT04936997); primary outcomes were immune responses with a secondary outcome of safety. At one week after a third immunization, 16 participants demonstrated a median 3-fold increase in neutralizing antibody responses, but no improvement was observed in T cell responses. Adverse events were mild. These results suggest that a third dose of BNT162b2 is safe, improves humoral immunity against SARS-CoV-2, and could be immunologically beneficial for cancer patients on active chemotherapy.

Introduction

The COVID-19 pandemic has led to over 200 million infections worldwide and claimed over 4 million lives to date. While non-pharmaceutical public health interventions managed to control outbreaks in some countries, most of the global population will depend upon vaccines to mitigate the pandemic. Since the identification of SARS-CoV-2 as the causative agent of COVID-19 in January 2020[1,2], vaccines with very high efficacy have been developed and deployed with remarkable speed. Independent clinical trials demonstrated 94–95% vaccine efficacy against symptomatic disease caused by SARS-CoV-2 for both the Pfizer/BioNTech and Moderna mRNA-based vaccines[3,4]. Based on these data, in December 2020, both the Pfizer/BioNTech and Moderna vaccines were granted emergency use authorization by regulatory agencies in North America.

These clinical trials, however, largely excluded immunocompromised individuals, including patients on immunosuppressive therapies to control chronic inflammatory conditions, primary immunodeficiencies, organ transplant recipients, and cancer patients on cytotoxic chemotherapy. Concern has been particularly high about the impact of COVID-19 on cancer patients since a study from the COVID-19 Cancer Consortium showed a 13% 30-day all-cause mortality from COVID-19 in a study of 928 patients, which is 10–30 times greater than that observed in the general population[5]. Importantly, the investigators noted a higher risk of death in patients with active cancer[5].

Several recent reports have shown diminished immune responses to SARS-CoV-2 infections and mRNA vaccines in subsets of immunocompromised patients, although these vary greatly with the nature of the immunosuppressive therapy[6–9]. For example, patients with autoimmune conditions or chronic lymphocytic leukemia treated with B cell-depleting antibodies have predictably diminished humoral responses to vaccination, whereas responses by patients on anti-TNFα therapies are less affected[6,7]. Notably, organ transplant recipients mount very poor antibody responses to the first mRNA immunization relative to healthy individuals[10], which increase somewhat after the second immunization[8]. Similarly, in cancer patients with solid or hematological malignancies, antibody responses are markedly diminished after the first immunization but improve somewhat after the second[9]. More data are required to instruct whether additional immunizations might further protect this vulnerable population.

Here we report on the serological and cellular immune responses following 2-dose BNT162b2 vaccination of solid tumor patients on active cytotoxic chemotherapy compared with healthy controls, and the outcomes of a Phase 1 trial of a third vaccine dose subsequently initiated in the cancer cohort based on our initial 2-dose results.

Results

Participant characteristics of control and cancer cohorts:

For the observational study (Table 1), 53 patients with a known diagnosis of a solid tumor malignancy on active immunosuppressive cancer therapy were enrolled through the University of Arizona Cancer Center during their routine care. The 50 participants in the control cohort of the observational study were enrolled through the State of Arizona's COVID-19 BNT162b2 vaccine point of distribution site at the University of Arizona during the phase 1B vaccination program while in the observational waiting area after their first dose. Table 1 summarizes chemotherapeutic regimens prescribed for the cancer cohort patients, with a full list in Supplementary Table 1. All eligible cancer cohort patients were subsequently invited to participate in an interventional trial to receive a third dose of vaccine (NCT04936997). Twenty patients were consented and participated in this interventional trial (Extended Data Figure 1). The primary endpoint for both of these studies was change in neutralizing antibody titers and all other immune biomarkers were secondary endpoints. Exploratory analyses include hierarchical clustering and age adjusted analyses.

Antibody responses to BNT162b2 vaccination:

Blood samples for serological and cellular analyses were collected several minutes after the first immunization, at the time of the second immunization 3 weeks later, and again 5–11 days after the second vaccination (Figure 1a). Peripheral blood mononuclear cell (PBMC) counts were similar between the cancer and control cohorts (Extended Data Figures 2a, Supplementary Figure). However, we noted a significant reduction in the frequency of CD19+ B cells and an increase in CD13+ myeloid cells in the cancer cohort relative to controls (Extended Data Figures 2b–c). Despite the overall reduction in the frequency of CD19+ B cells in the cancer cohort, naive and other activated subsets were well-represented within these B cells (Extended Data Figure 2d, Supplementary Figure). Using serum from each of these samples, we first obtained single-dilution semi-quantitative data on Spike protein-specific antibody levels. Of control cohort participants, using a University of Arizona clinical serology test[11], four tested as positive for prior SARS-CoV-2 exposure at the first blood draw and were excluded from further analyses. Four cancer cohort participants self-reported prior COVID-19 but did not display serological evidence of prior infection and were not excluded. For both the control and cancer cohorts, we observed progressive increases after the first and second vaccinations in antibodies specific for the S2 region of Spike protein (Figure 1b). This region contains several antibody epitopes that are conserved across other common human β-coronaviruses[12–16], including at least one weakly neutralizing epitope[17,18]. Although both the cancer and control cohorts showed responses, median S2-specific antibody values were diminished in cancer patients relative to the control cohort at matched timepoints (Figure 1b). As most neutralizing and protective antibodies are directed to the receptor binding domain (RBD) of Spike protein[19,20], we also semi-quantitatively determined the relative levels of these antibodies. Increases were also seen for RBD antibodies in both the healthy and cancer cohorts after each vaccination (Figure 1c). Yet, as with antibodies against S2, the levels of RBD antibodies at draws 2 and 3 post-vaccination in the cancer cohort were diminished relative to healthy controls (Figure 1c). To obtain more quantitative information, we performed a full dilution series

to determine antibody titers against RBD (Extended Data Figure 2e). Consistent with the semi-quantitative results, RBD antibody titers increased after the second immunization in both groups, but the median titers observed in the cancer cohort were reduced by >11-fold relative to healthy controls (Figure 1d). Seven of the cancer cohort, but none of the control cohort, failed to generate RBD-specific antibody titers above the limit of detection.

For most vaccines, neutralizing antibody titers are the best correlate of protection from infections[33]. We therefore directly assessed antibody-mediated neutralization of authentic live SARS-CoV-2 (WA1 isolate) after the first and second immunizations. After the first shot, we observed a median plaque reduction neutralization test (PRNT)-90 titer of 60 in the control cohort and 20 in the cancer cohort (Figure 2). However, whereas all but one participant in the control cohort showed detectable virus neutralizing activity, this was observed in only 67% of the cancer cohort (Figure 2). After the second immunization, all healthy controls had virus-neutralizing antibodies, with a median PRNT90 titer of 540 (Figure 2). In contrast, 80% of the cancer cohort had detectable neutralizing antibodies with a median titer of 60 (Figure 2). Virus-neutralizing titers correlated with overall RBD-specific antibodies (Extended Data Figure 3). These results demonstrated that most of the cancer cohort generated protective antibodies, but at levels well below that of the control cohort after the second vaccine dose. We did not find any obvious clinical characteristics that would have modified the relationship between immunosuppression and vaccine response. Of the non-responders, 60% were breast cancer patients, 90% were female and the median age was 64. While there is no statistical power to compare this subgroup to the overall cancer cohort, the only obvious difference was treatment timing (Table 1), as the average time between treatment and vaccine dose 2 was over 2 weeks in the overall group compared to less than 1 week in non-responders.

T cell responses to BNT162b2 vaccination:

Prior studies have found that potentially protective T cell responses can be observed in COVID-19 convalescent individuals and in animal models when antibody levels are very low, such as after asymptomatic infections[21–24]. To quantify T cell responses in our healthy and cancer cohorts, peripheral blood mononuclear cells (PBMCs) were cultured overnight with either activating anti-CD3 antibodies (Extended Data Figure 4a) or a pool of overlapping Spike protein peptides capable of presentation on both HLA-I and HLA-II (Figure 3a). ELISPOT assays were then performed to quantify interferon gamma (IFNγ)-producing T cells relative to paired control wells in which no peptides were added. In the control cohort, we observed a marked increase in the median frequency of IFNγ+ T cells after the first vaccination relative to pre-vaccination timepoints (2.9 fold, p=0.02), and a further increase after the second vaccination (2.6 fold, p=0.0003, Figure 3a). Within the cancer cohort, the first vaccination did not induce a statistically significant increase in the median frequency of Spike-specific IFNγ+ T cells at draw 2, but a clear increase was observed at draw 3 (4-fold, p=0.0007, Figure 3a), though there was substantial variability in the response. T cell frequencies in the cancer approached but remained below the levels observed in the control cohort after the second vaccination (p=0.03, Figure 3a). To estimate CD8+ and CD4+ T cell contributions, we re-tested samples with the highest Spike-specific T cell frequencies in the presence or absence of blocking antibodies against

HLA-I and/or HLA-II, respectively. Substantial variation was observed across individuals in both the control and cancer cohorts, especially in HLA-I-dependent CD8+ T cell responses (Extended Data Figure 4b). Nonetheless, the data indicate that most individuals mount both CD4+ and CD8+ T cell responses.

To determine whether participants with poor neutralizing antibody titers might be partially protected by T cell responses, we examined T cell frequencies grouped by neutralizing antibody titers. Spike protein peptide-specific T cell frequencies at draw 1 were subtracted from the final draw 3 numbers to define individuals who mounted a response to vaccination. As has previously been described in post-infection responses[21,25], Spike protein peptide-specific T cell frequencies correlated relatively poorly with neutralizing antibody titers for both the healthy and cancer cohorts (Figure 3b). These data revealed that 4/10 cancer patients had detectable T cell responses even when PRNT90 titers were undetectable (Figure 3b). Thus, despite chemotherapy-induced immune suppression, relatively few cancer patients failed to make any detectable neutralizing antibody or T cell response. Nonetheless, these responses were substantially diminished relative to the control cohort, likely due to anti-cancer therapy.

One drawback to these interpretations is that the median age of the cancer cohort was greater than that of controls (Table 1). This raises concerns that some of the differences we observed were effects of age rather than of anti-cancer therapy. Yet the only immunological parameter that showed an age-dependent effect was anti-RBD antibody levels, which did show a decline with increasing age in the control cohort ($p_{interaction} = 0.01$, Extended Data Figure 5a). However, we observed no such age-dependent differences in the cancer cohort. Moreover, no other immunological parameters such as neutralizing antibody levels or T cell responses were altered as a function of age (Extended Data Figure 5b–c). Furthermore, when limiting the data to participants > 39 years of age (upper three quartiles), the differences between the two cohorts remained statistically significant for all immunological parameters (RBD antibodies $p<0.0001$; neutralizing antibodies $p<0.0001$; Spike-specific T cells $p=0.04$). These data are consistent with the only modest age-dependent effects in immune responses reported in BNT162b2 phase 1 clinical trials[26].

Because we assessed responses between 5–11 days after the second immunization, we examined whether there were any time-dependent changes in responses within this window. RBD-specific antibodies, neutralizing titers, and T cell responses did not obviously differ as a function of time after vaccination (Extended Data Figure 6a). Most control and cancer cohort participants were tested at 7–8 days after vaccination (Extended Data Figure 6a). Although the study was not powered for subgroup analyses, we also examined whether the tumor subtype might influence immune responses. No obvious differences were observed in antibody and T cell responses between breast, pancreatic, and other tumor types (Extended Data Figure 6b). We noted that one participant in the cancer cohort mounted a much stronger antibody response than the rest of the group (Extended Data Figure 6a–b). This participant had self-reported prior COVID-19 infection, despite seronegativity prior to the first immunization. Yet three other cancer cohort participants with self-reported prior COVID-19 showed no unusual patterns of antibody or T cell responses (Extended Data Figure 6c). Based on our initial inclusion criteria of seronegativity prior to vaccination, we

retained these individuals in our analyses, but note that at least one of these four participants might be mounting recall, rather than primary responses. Together, these data suggest that anti-cancer therapy hampers immune responses to the COVID-19 vaccine BNT162b2. The effectiveness of these diminished immune responses in preventing COVID-19 is presently unknown.

Memory B cell subsets after BNT162b2 vaccination:

Memory B cell frequencies are predictive of anamnestic responses following booster vaccination[27], and presumably viral exposures. We first quantified RBD-specific CD19+ B cells in the control and cancer cohorts using antigen tetramers (Figure 4a). We also simultaneously measured memory B cells that bound the S1 region of spike protein but not RBD (Figure 4a), as the N-terminal domain of S1 contains a potent neutralizing epitope[28,29]. S2 tetramer reagents yielded high flow cytometric background staining of naïve B cells and myeloid cells and were thus not used to further define antigen-specific memory lymphocytes (data not shown). Within the control cohort, a clear increase in total RBD-specific B cells was observed after vaccination, but no statistically significant increase was observed in such cells in the cancer cohort (Extended Data Figure 7). Neither the control nor the cancer cohort showed a significant increase in S1-specific B cells with vaccination (Extended Data Figure 7).

To gain more resolution, we examined antigen-specific frequencies within defined memory B cell subsets. These subsets exhibit different behaviors in recall responses, generating either plasmablasts or new germinal centers[30–36]. These lineage potentials correlate with antibody isotype and other markers[30–36]. We therefore quantified RBD- and S1-specific naive B cells, plasmablasts, and memory B cell subsets after vaccination[35,37–39]. These subsets include IgG+ and IgM+ CD27+ CD21+ classical resting memory B cells, CD27+ CD21- CD11c+ pre-plasmablast memory B cells, CD27- IgD- CD11c- CD21+ DN1 cells, CD27- IgD- CD11c+ DN2 cells, and CD27- IgD- CD11c- CD21- DN3 cells (Figure 4a, Supplementary Figure). In the control cohort, we observed a clear increase in the frequency of isotype-switched RBD-binding CD21+ classical resting memory B cells as well as CD21- pre-plasmablast memory B cells after each vaccination (Figure 4b). Isotype-switched S1-binding CD21- memory B cells were also observed to increase after each vaccination of the control cohort (Figure 4b). After the second vaccine dose in the cancer cohort, we also observed increases in the mean frequencies and/or rates of change of isotype-switched RBD- and other S1-specific pre-plasmablast CD21- memory B cells, but the median levels were ~10-fold lower than those observed in the control cohort (Figure 4b). We were unable to detect isotype-switched RBD- or S1-specific classical resting memory B cells above pre-vaccination levels in the cancer cohort (Figure 4b). Some other RBD- and S1-binding memory B cell subsets were detectable in the healthy and cancer cohorts, but in general the frequencies of these cells were substantially lower than the isotype-switched CD27+ subsets and not consistently increased with each immunization (Extended Data Figure 8). We were unable to detect antigen-specific cells above background levels in naive B cells (Extended Data Figure 8). Thus, RBD- and S1-specific B cells early after vaccination are enriched in IgG+ memory subsets. These cells are biased towards plasma cell fates[33,35], though secondary germinal centers could conceivably arise from classical

CD21+ memory cells[34]. In both cohorts, we observed increases in RBD-specific antibody-secreting plasmablasts, with no statistically significant differences between cohorts (Figure 4b). S1-specific plasmablasts were not readily apparent in either group (Figure 4b). This might be partly due to poor survival of plasmablasts after freezing and in part due to lower surface B cell receptor levels[40].

We next examined whether RBD- and S1-specific memory B cells could be detected in cancer patients with no or low levels of neutralizing antibodies. Prior studies have shown that memory B cell numbers and specificities correlate only modestly with serum antibodies[36,41–44]. CD21- RBD+ and S1-specific memory B cell frequencies at draw 3 were added to DN2 and DN3 RBD+ memory B cell frequencies for each cancer patient, as these subsets were the only ones in which cancer patients consistently showed vaccine-induced increases (Figure 4b and Extended Data Figure 8). Next, the corresponding pre-vaccination draw 1 frequencies were subtracted to correct for background levels in each patient. These net memory B cell frequencies were then plotted as a function of virus neutralization titers. Patients without detectable neutralizing antibodies also generally lacked RBD- and S1-specific memory B cells (Figure 4c). In contrast, patients with modest but detectable neutralizing antibody titers consistently showed RBD- and S1-specific memory B cells after the second immunization (Figure 4c). These data suggest that patients with low but detectable Spike-specific antibodies would likely generate anamnestic responses after a third immunization, conceivably approaching levels seen in healthy controls after the second vaccination.

Responses of cancer patients to a third dose of BNT162b2:

To directly determine whether and how immunity can be improved by a third vaccination, we initiated an interventional trial for our cancer cohort. Twenty of the original cohort agreed to participate and met the inclusion criteria (Methods). Participants were not informed of their immune response results. There were no statistically significant associations between participation and draw 3 RBD-specific antibodies, neutralization titers, or Spike-specific T cells. However, we note the study was not powered sufficiently to specifically preclude these differences. All patients were contacted within 2–4-week windows for adverse events. There were no Serious Adverse Events (SAEs) noted (Figure 5a), with 9 (45%) participants experiencing injection site pain. Other minor Adverse Events (AEs) included: generalized myalgia (15%); bone pain (5%); fatigue (10%); chills (10%); and appetite loss (5%). There were no obvious demographic differences between the 20 participants and the original cancer cohort; however, these participants did have a shorter window between administration of cancer treatment and blood draws for analyses. Patients in this cohort had gastrointestinal cancers predominantly (75%) compared with 51% in the original cancer cohort; the remaining five participants (25%) had a breast cancer diagnosis compared to 42% in the original cancer cohort.

Blood samples were collected at the time of the third vaccine dose (Draw 4, Extended Data Figure 9a) and 1 week afterwards (Draw 5). RBD-specific antibodies, virus-neutralizing antibodies, and Spike-specific T cells were quantified. A modest but consistent and statistically significant increase from Draw 4 to Draw 5 was observed in mean RBD-specific

antibody titers (0.49 vs. 0.72, p=0.0005, Figure 5b). This was accompanied by a 3-fold increase in median virus-neutralizing antibody titers (60 vs. 180, p=0.01, Figure 5c). Interestingly, two participants who had no detectable neutralizing antibodies at Draw 3 showed an increase at Draw 4, even prior to the third immunization (Figure 5c). In both cases, neutralizing antibodies increased further after the third shot (Figure 5c). We observed no overall increase in T cells after booster immunization of the cancer cohort (Figure 5d). Because participants received the third shot between 42–111 days after the third blood draw, we examined whether the duration of time between immunizations might influence the magnitude of the antibody response, as has been reported for doses 1 and 2[45]. Yet we observed no correlation between the time between doses and the magnitude of the RBD-specific or neutralizing antibody recall responses in this small cohort (Extended Data Figures 9b–c).

Prior studies of vaccinations of COVID-19 convalescent individuals revealed a strong correlation between pre-existing memory B cells and the magnitude of the antibody response after immunization[27]. To determine whether such a relationship could be observed in our cancer cohort, we plotted the draw 3 RBD-specific memory B cell frequencies (switched CD21-, switched CD21+, DN2, and DN3) against the change in RBD-specific antibodies after the booster immunization. Unexpectedly, we observed no correlation between these parameters (Extended Data Figure 9d). A similar lack of correlation was observed between summed RBD and S1-specific memory B cells and boosted virus-neutralizing antibody titers (Extended Data Figure 9e). These data suggest that unlike in healthy individuals[27], memory B cell frequencies are not quantitatively predictive of the magnitude of the antibody response in our cancer cohort.

To begin to explain this lack of correlation between memory B cells and subsequent anamnestic responses, we performed comparisons of memory B cell frequencies, antibody levels, and T cell responses prior to the third vaccine dose at draw 3 (Extended Data Figure 10). Most parameters were well-correlated with each other in the control cohort in biologically rational ways. For example, isotype-switched CD27+ and DN2 subsets clustered together and were highly correlated (Extended Data Figure 10). Within the cancer cohort, however, memory B cell subsets were not well-correlated and did not cluster with each other (Extended Data Figure 10). This suggests a lack of coordination between aspects of the response that are normally linked, which in turn may lead to quantitatively unpredictable recall responses. Nonetheless, antibody responses did improve in most cancer patients who received a third vaccine dose.

Discussion:

The COVID-19 pandemic has dramatically affected the world, with a profound impact on cancer patients and their care. Thus, the development of COVID-19 vaccines was anxiously awaited in the cancer community. Given that none of the COVID-19 vaccine trials included patients with active malignancies[3], the efficacy of these vaccines in solid tumor patients on active therapy was not reported. While prior studies in patients with colorectal and breast cancers on active chemotherapy who receive influenza vaccination show that patients can mount a serological response, the immunogenicity of the COVID-19 vaccines

in these patients is largely unknown[46,47]. A recent study of 658 organ transplant recipients demonstrated a lower antibody response after two doses of the BNT162b2 COVID-19 vaccine when compared to immunocompetent study participants[8]. Similarly, one study suggested that cancer patients do not mount the same antibody responses to the BNT162b2 vaccine as healthy controls[9].

Our results agree with certain aspects of these findings: as with a recent study on immunocompromised cancer patients[9], we observed lower overall antibody and T cell responses in cancer patients compared with control cohorts. Yet in contrast to the prior results, we observed that the majority of our patients seroconverted after the first immunization, as measured by live virus neutralization assays. This frequency further increased after the second vaccination. These differences could potentially be explained by the nature of our cohort, which did not include patients on immunotherapy or patients with hematologic malignancies. In addition, neutralization assays using authentic viral isolates, as we used here, tend to be more sensitive than experiments performed with Spike protein-pseudotyped lentiviruses[11,48].

It is encouraging that we also observed T cell responses in most vaccinated cancer patients, including nearly half that mounted undetectable neutralizing antibody responses. Unlike antibodies, these T cell responses were only modestly reduced relative to the control cohort. Of note, many individuals possess Spike-reactive memory T cells, but not B cells or antibodies, even prior to SARS-CoV-2 exposure or vaccination[49–53]. It is possible that these pre-existing coronavirus cross-reactive memory T cells dominate after vaccination, diminishing the negative impact of anti-cancer therapy on immunization. The resulting CD4+ T cells could potentially help naive B cells participate in subsequent responses to vaccines and infections, which may help explain the poor correlations we observed between memory B cell frequencies and the magnitude of the recall responses in cancer patients. Given that T cells reduce viral loads and disease even when neutralizing antibody levels are low[21,23,24,54], these data suggest that vaccination may confer at least partial protection and reduce the likelihood of severe COVID-19 in most cancer patients.

Nonetheless, when compared with individuals not on immunosuppressive therapy, the magnitudes of vaccine-induced antibody and T cell responses were substantially reduced in cancer patients. These reduced levels may be particularly problematic when faced with variants possessing some neutralizing antibody-evading mutations, such as beta, gamma, or delta[55,56]. Some participants in our cohort failed to mount detectable antibody or T cell responses by 1 week post-immunization, although several did show improvement over time. This seems likely to diminish vaccine effectiveness relative to the benchmark of 94–95% in non-immunocompromised populations[3,4].

Several recent studies have reported improved antibody responses in transplant recipients after a third dose, though neutralizing antibodies and T cells were not quantified[57,58]. We therefore initiated a trial to determine whether a third immunization would improve immunity in our cohort on active anti-cancer therapy. Interestingly, two participants who initially failed to mount detectable responses by 1 week after the second vaccination later displayed detectable antibodies prior to the third dose; one patient with cholangiocarcinoma

and another with pancreatic cancer. This suggests that for at least a subset of the non-responding cancer cohort, antibody responses may be delayed but not completely absent. After the third immunization, neutralizing antibody levels improved in 16 out of 20 participants. In all but one of the participants who improved, neutralizing antibody titers reached 180 or greater. In non-human primate and modeling studies, this level is protective against disease[24,59,60]. Nonetheless, the overall antibody increases induced by the booster immunization were fairly modest, and, for reasons that are unclear, no further improvement was observed of circulating Spike-specific T cell frequencies.

Our cancer cohort naturally had an expected heterogeneity in terms of cancer diagnoses, the types of cytotoxic therapy patients received, and the timing of these therapies relative to vaccine dose. Thus, it is difficult to draw conclusions related to which solid tumors were associated with a better vaccine response or which therapies correlated with the non-responders. Yet it is worth noting that most of the initial non-responders had blood collected for immune analysis 7–14 days after their most recent treatment with cytotoxic agents. This time course is aligned with a nadir in blood counts and the peak of myelosuppression from traditional chemotherapy agents. While the numbers are too small to draw strong conclusions, these findings are certainly hypothesis-generating and merit further exploration to better understand the ideal timing for vaccination in patients on active immunosuppressive therapy. Our cancer cohort was also on average older than participants in the control cohort. There did appear to be an age-moderated effect within the control group on anti-RBD titers, which in turn could impact the magnitude of the differences we observed between the control and cancer cohorts. Yet no other immunological parameters were similarly affected and we did not observe age-moderated effects within the cancer cohort for any immunological parameter. Thus, the major driver of diminished responses in the cancer cohort is likely to be anti-cancer therapy rather than age.

Together, our data suggest that most cancer patients on active chemotherapy are likely to exhibit improved antibody levels, which has been correlated with protection against disease[59,60], after a third immunization. Yet given the relatively modest increases in antibodies and recalcitrance of T cells, expectations should remain tempered as to the degree of benefit. Quantitative antibody tests can potentially be used to select individuals who need and would most benefit from a booster.

Methods:

Participant Selection:

Recruitment for both the healthy cohort and cancer cohort was approved by the University of Arizona Institutional Review Board in January 2021. The interventional amendment to the protocol and subsequent enrollment for a third shot in cancer patients was activated in June 2021 (NCT04936997). Participants were recruited to the control cohort during the Phase 1B Pima County COVID-19 vaccine rollout. Participants scheduled for vaccine appointments at Banner University Medical Center North site were approached with the IRB-approved consent and sequentially enrolled. Thereafter, patients with cancer diagnosis were enrolled at the University of Arizona Cancer Center. Informed consent was obtained for all participants and participants were aware they would not be informed of their specific immune results.

No compensation was offered for participation. Eligible solid tumor cancer patients had to have active disease and be receiving ongoing cytotoxic systemic therapy. Patients receiving immunotherapy were excluded. Demographic information was collected in addition to cancer diagnosis and type of anti-cancer therapy. Dates of last treatment prior to vaccine administration were also noted. In total, 73 control cohort participants were consented and 65 completed all three blood draws and both vaccine shots; five did not come in for their blood draw and eleven did not show up for their scheduled vaccinations. Fifty-six cancer patients were consented for the study and 53 completed all three blood draws and received both shots. Vaccine doses were administered while patients were receiving cytotoxic therapy and this treatment was not interrupted for vaccine administration. All of the cancer cohort participants received the Pfizer vaccine, BNT162b2, 61 enrolled participants in the control cohort received the Pfizer vaccine and 12 received the Moderna vaccine, mRNA 1273. For consistency, analyses are restricted to those participants that received the BNT162b2 vaccine. There were four control cohort participants that were seropositive based on the University of Arizona COVID-19 ELISA pan-Ig Antibody Test[11]; all of these participants were removed from analyses. The complete study sample size is 53 cancer cohort patients and 50 control cohort participants.

For the interventional booster all 53 patients in the cancer cohort were considered for continued eligibility and re-consenting and 38 did not participate. Specific reasons for lack of participation included: eleven participants ineligible due to going off chemotherapy (11.3%); ten died (unrelated to vaccine as per clinical provider) or were in hospice (19%); six had clinical provider concerns regarding participation (11.3%); and eleven declined to participate (11.3%). The full CONSORT flow diagram is shown in Extended Data Figure 1. Blood samples were drawn for analysis prior to the administration of a third booster dose of the Pfizer mRNA vaccine. A final blood draw was performed on all 20 patients between 5–11 days from the time of the 3rd vaccine. Enrollment of the first patient was on 6/8/2021 and the final patient was enrolled on 6/25/2021. Patients in this cohort were contacted at 2 weeks (+/− 3 days) and 4 weeks (+/− 7 days) post booster dose for adverse events and serious adverse event monitoring. All cancer patients who were included in the observational study (n=53) were evaluated for inclusion into the interventional study and there were no interim analyses performed. The per protocol analyses was to recruit from the 53 evaluable participants from the observational study. This number of participants was unknown at the time of initial IRB evaluation of the protocol and a placeholder of n=1000 was included. The University of Arizona Cancer Center (UACC) Data Safety and Monitoring Board (DSMB) was the DSMB of record for the interventional component of the trial. The trial was monitored and reviewed for safety quarterly as it was determined to be a low-risk study per the UACC DSMB charter. The trial protocol is included in the Supplementary Appendix.

Peripheral blood mononuclear cell and serum preparation:

Twenty mL of blood was collected by venipuncture in heparinized Vacutainer tubes (BD) and an additional 10 mL was collected in clot activating non-heparinized Vacutainer tubes. After >30 minutes at room temperature, non-heparinized tubes were spun at 1200 × g for 10 minutes, and serum was collected and frozen in 1 mL aliquots at −20°C. For peripheral

blood mononuclear cells (PBMCs), 15 mL of Ficoll-Paque Plus (Fisher Scientific) was added to 50 ml Leucosep tubes (Greiner) and spun for 1 minute at 1000 × g to transfer the density gradient below the filter. Twenty mL of blood from the heparinized tubes were then poured into the top of the Leucosep tube and then spun at 1000 × g for 10 minutes at room temperature with the brake off. The top plasma layer was carefully collected and frozen at −20°C and the remaining supernatant containing PBMCs above the filter was poured into a new 50 mL conical tube containing 10 ml phosphate buffered saline (PBS) and spun at 250 × g for 10 minutes. Cell pellets were resuspended in RPMI media containing 10% fetal calf serum and counted on a ViCell XR (Beckman Coulter). Cells were resuspended to a concentration of 2×10^7 cells/mL in RPMI media containing 10% fetal calf serum. An equal volume of 80% fetal calf serum + 20% dimethyl sulfoxide was added dropwise and inverted once to mix. Suspensions were distributed at 1 mL/cryovial and frozen overnight at −80°C in Mr. Frosty freezing chambers (Nalgene). Vials were then transferred to storage in liquid nitrogen.

ELISAs and quantification of antibody titers:

Serological assays were performed as previously described. RBD was purchased from GenScript (catalog # Z03483) and S2 subdomain of the SARS-CoV-2 S glycoprotein was purchased from Sino Biological (catalog # 40590-V08B). To obtain titers and single-dilution OD450 values, antigens were immobilized on high-adsorbency 384-well plates at 5 ng/ml. Plates were blocked with 1% non-fat dehydrated milk extract (Santa Cruz Biotechnology #sc-2325) in sterile PBS (Fisher Scientific Hyclone PBS #SH2035,) for 1 h, washed with PBS containing 0.05% Tween-20, and overlaid for 60 min with either a single 1:40 dilution or 5 serial 1:4 dilutions beginning at a 1:80 dilution of serum. Plates were then washed and incubated for 1hr in 1% PBS and milk containing anti-human Pan-Ig HRP conjugated antibody (Jackson ImmunoResearch catalog 109–035-064) at a concentration of 1:2000 for 1 h. Plates were washed with PBS-Tween solution followed by PBS wash. To develop, plates were incubated in tetramethylbenzidine prior to quenching with 2N H2SO4. Plates were read for 450nm absorbance on CLARIOstar Plus from BMG Labtech. All samples were also read at 630nm to detect any incomplete quenching. Any samples above background 630nm values were re-run. Area Under the Curve values were calculated in GraphPad Prism (v9).

T cell assays:

Frozen PBMCs were thawed by mixing with 10 mL of pre-warmed RPMI 1640 media (Gibco) containing 10% fetal calf serum (Peak Serum #PS-FB1), 1X Penicillin-Streptomycin (HyClone #SV30010) and 0.03 mg/mL DNAse (Sigma #DN25–100) in a 15 mL conical tube and spun at 540 × g for 5 minutes. Cell pellets were resuspended in 1 mL of X-VIVO 15 media with Gentamicin and Phenol Red (VWR #12001–988) containing 5% male human AB serum (Sigma #H4522–100ML), and incubated in 24-well plates overnight at 37°C with 5% CO2. 250 μL of each sample was plated on a 96-well round bottom plate and spun at 540 × g for 3 minutes, and then resuspended in 150 μl X-VIVO 15 media with 5% male human AB serum containing either 0.6 nmol PepTivator SARS-CoV-2 Prot_S peptide pool (Miltenyi Biotec #130–126-701) for antigen specific T cell stimulation, or positive control anti-CD3 mAb CD3–2 from Human IFN-γ ELISpot plus kit (Mabtech #3420–4APT-2), or blank media as negative control. In some experiments, 10 μg/ml

blocking antibodies against HLA-I (W6/32, Biolegend) and/or HLA-II (Tü39, Biolegend) were included. Antibodies were validated by the manufacturer on human peripheral blood mononuclear cells. Cell suspensions were transferred to pre-coated IFN-γ ELISpot plates and incubated overnight at 37°C with 5% CO2. Plates were emptied, washed 5 times with 200 μl/well of PBS (Fisher Scientific Hyclone PBS #SH2035), and incubated for 2 hours at room temperature with 100 μl/well PBS containing 0.5% fetal calf serum and 1 μg/ml detection antibody (7-B6–1-biotin). Plates were washed as above and incubated for 1 hour at room temperature with 100 μl/well of PBS-0.5% FCS with 1:1000 diluted Streptavidin-ALP. Plates were washed as above and developed for 10–15 minutes with 100 μl/well substrate solution (BCIP/NBT-plus) until distinct spots emerged. Color development was stopped by washing extensively in tap water and left to dry. Spots were imaged and counted using an ImmunoSpot Versa (Cellular Technology Limited, Cleveland, OH) plate reader.

Virus neutralization assays:

All live virus assays were performed at BSL-3. SARS Coronavirus 2, Isolate USA-WA1/2020 (BEI NR-52281) was passaged once on Vero (ATCC #CCL-81) cells at a multiplicity of infection of 0.01 for 48 hours. Supernatant and cell lysate were combined, subjected to a single freeze-thaw, and then centrifuged at 1800 × g for 10 minutes to remove cell debris. For plaque reduction neutralization tests (PRNT) for SARS-CoV-2, Vero cells (ATCC # CCL-81) were plated in 96-well tissue culture plates and grown overnight. Vero cells were PCR-confirmed to be mycoplasma-free. Serial dilutions of serum samples were incubated with 100 plaque forming units of SARS-CoV-2 for 1 hour at 37°C. Plasma/serum dilutions plus virus were transferred to the cell plates and incubated for 2 hours at 37°C, 5% CO2 then overlaid with 1% methylcellulose. After 72 hours, plates were fixed with 10% Neutral Buffered Formalin for 30 minutes and stained with 1% crystal violet. Plaques were imaged using an ImmunoSpot Versa (Cellular Technology Limited, Cleveland, OH) plate reader. The most dilute serum concentration that led to 10 or fewer plaques was designated as the PRNT90 titer.

Flow cytometry:

One mL of pre-warmed fetal calf serum was added to a frozen cryovial of PBMCs which was then rapidly thawed in a 37°C water bath. Samples were poured into 15 mL conical tubes containing 5 mL pre-warmed RPMI + 10% fetal calf serum and spun at 250 × g for 5 minutes, room temperature. Supernatants were removed and pellets were washed once with 500 ul PBS containing 5% adult bovine serum and 0.1% sodium azide (staining buffer). Cell pellets were then resuspended in 200 μl staining buffer containing 1μl each of anti-IgM-FITC (Biolegend clone MHM-88), anti-IgD-PerCP-Cy5.5 (Biolegend clone IA6–2), anti-CD11c-Alexa700 (Biolegend clone Bu15), anti-CD13-PE-Cy7 (Biolegend clone WM15), anti-CD19-APC-efluor-780 (eBioscience clone HIB19), anti-CD21-PE-Dazzle (Biolegend clone Bu32), anti-CD27-BV510 (Biolegend clone M-T271), anti-CD38-APC (Biolegend clone HIT2), RBD-PE tetramer, and S1-BV421 tetramer. Antibodies were validated by the manufacturer on human peripheral blood mononuclear cells. Tetramer reagents were assembled by mixing 100μg/ml C-terminal Avitagged RBD or S1 (AcroBiosystems) with 100μg/ml streptavidin-PE (eBiosciences) or streptavidin-BV421 (Biolegend), respectively, at a 5:1 molar ratio in which 1/10 the final volume of streptavidin was added every 5 minutes.

S1 and RBD tetramers were validated by staining Lenti-X 293T cells (Takara Bio) as a negative control or 293T-hACE2-expressing cells (BEI Resources NR-52511) as a positive control. Lenti-X 293T cells were confirmed to be mycoplasma free; 293T-hACE2 cells were maintained in media containing 10μg/ml ciprofloxacin to minimize the chances of mycoplasma contamination. PBMC samples were stained for at least 20 minutes, washed, and filtered through 70 μm nylon mesh. Data were acquired on either a BD LSR2 or Fortessa flow cytometer. Data were analyzed using FlowJo software.

Statistical methods:

The primary statistical endpoint for the observational study was the change in antibody-mediated neutralization of authentic live SARS-CoV-2 PRNT90 titers from baseline to draw 3 between participants in the control cohort and cancer cohort. This primary endpoint, powered as a non-inferiority hypothesis, was whether vaccine-acquired PRNT90 titers were the same in immunocompromised patients compared to healthy individuals. These methods typically require estimating the outcome under a non-inferiority margin; however, this criterion is not necessary given the obvious superiority PRNT90 titers seen in healthy participants compared to cancer patients at draw 3. The primary endpoint for the interventional third vaccine dose study was the paired difference, using a paired t-test statistic, between draw 4 (booster shot) and draw 5 (7 days post-booster) with secondary analyses examining the paired difference in RBD titers (as AUC) and Spike-specific T cells. Secondary analyses for the observational study included comparing differences in slope and between blood draws, e.g. draw 1 to draw 2 and draw 2 to draw 3 between cohorts using repeated measures analysis of variance (ANOVA) that adjusts for the correlation within an individual by use of an exchangeable covariance matrix and F-test statistics. Pairwise differences between and within cohorts and draw were evaluated using two-way ANOVA and two-sided Sidak-adjusted t-test statistics. Additionally, analysis of covariance was used to evaluate whether age moderated the between cohorts draw 3 differences for the semi-quantitative 1:40 serum dilution ELISA for RBD and S2 spike proteins as well as RBD AUC and neutralizing Ab titers. The cancer cohort was older, on average, with a mean age of 64 years compared to 42 in the control cohort. The possible mediating effect of age on the immunologic response seen between the cohorts was evaluated in two ways. First, age was added as an interaction effect to draw 3 differences between cohorts, using linear models with age as a continuous variable. Additionally, since the primary age difference between cohorts was the lack of participants in the lowest age quartile (< 38 years of age) in the cancer cohort, the draw 3 differences were tested after removing this age group from the control cohort, thus removing the lower age bias that could have been introduced by including these participants; this resulted in a much smaller sample size in the control cohort (n = 23) and was performed using linear modeling with a two-sample, two-sided, t-test at the 0.05 level of significance.

For the interventional booster trial, the primary endpoint was the paired change in log10(PRNT90) from the interventional baseline titer (draw 4 since start of the observational study) to 1 week post-third BNT162b2 dose (draw 5). The primary hypothesis was that there would be an increase in log10(PRNT90) levels between these two blood draws. The test statistic was a two-sided paired t-test. A sample size of at least 35 participants

would achieve a power of 0.80 to detect a pairwise difference of 1.17 log10(PRNT90) at a 0.05 level of significance; this sample size assumes a pairwise SD of 2.39 as seen in the observational study. Secondary endpoints would include neutralizing antibodies, RBD titers, and T cell ELISPOTs. The intended sample size was not met for the reasons described in the Participant Selection section. Thus, the final cohort size for the interventional trial was 20.

All analyses were performed in GraphPad Prism 9 and/or the R programming language version 4.0.5.

Data Availability Statement:

Data are available in the main text, figures, extended data, and supplemental files. Raw immune biomarker data is provided in Supplementary Table 2 with individual identifying information removed to preserve patient confidentiality. Flow cytometric files can be requested by contacting D.B. Serum sample requests should be sent to D.B. and will be made available pending sufficient remaining quantities and completion of a Materials Transfer Agreement.

Extended Data

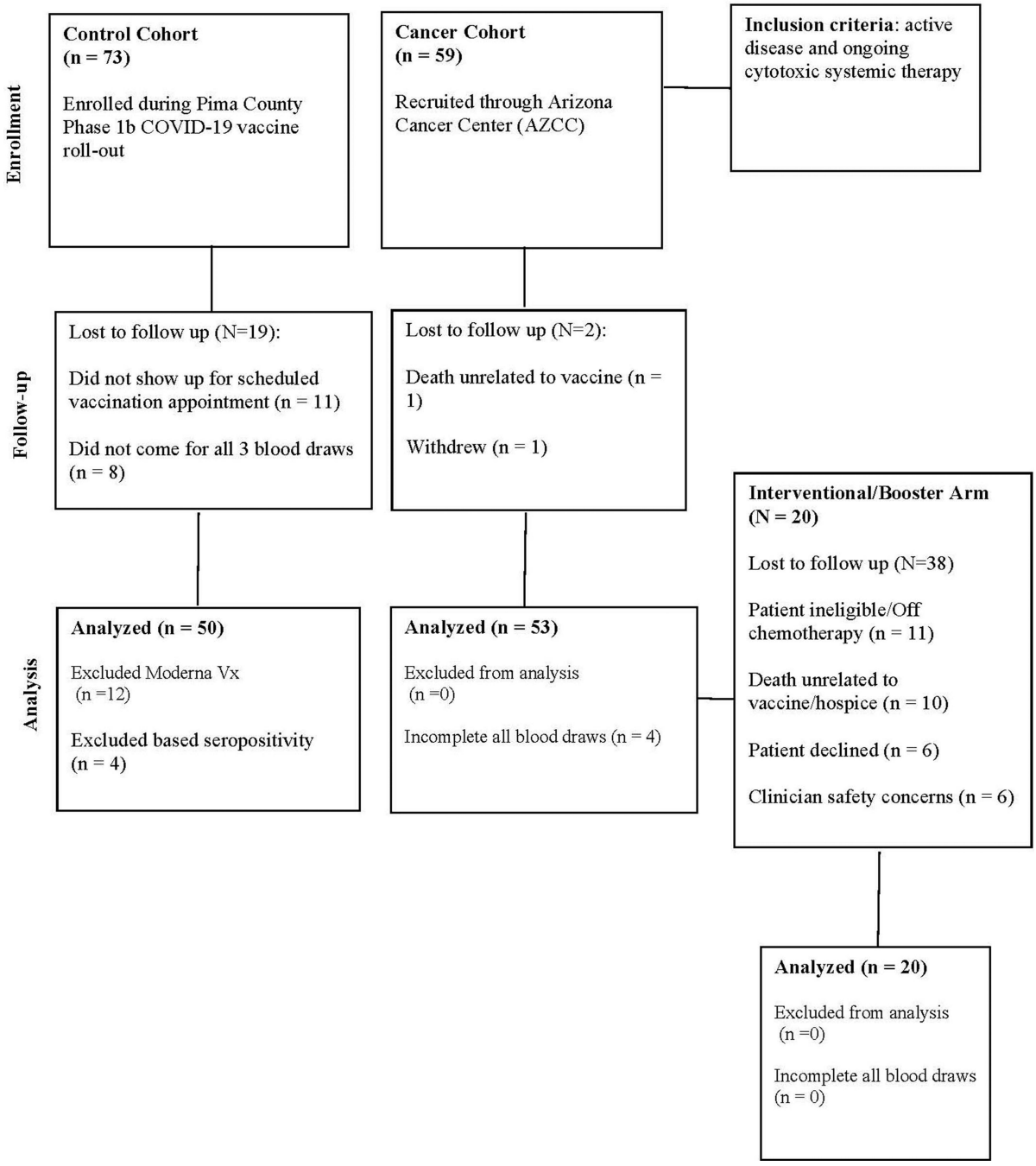

Extended Data Fig. 1. Consort Diagram.
Observational and Interventional (Booster) Studies.

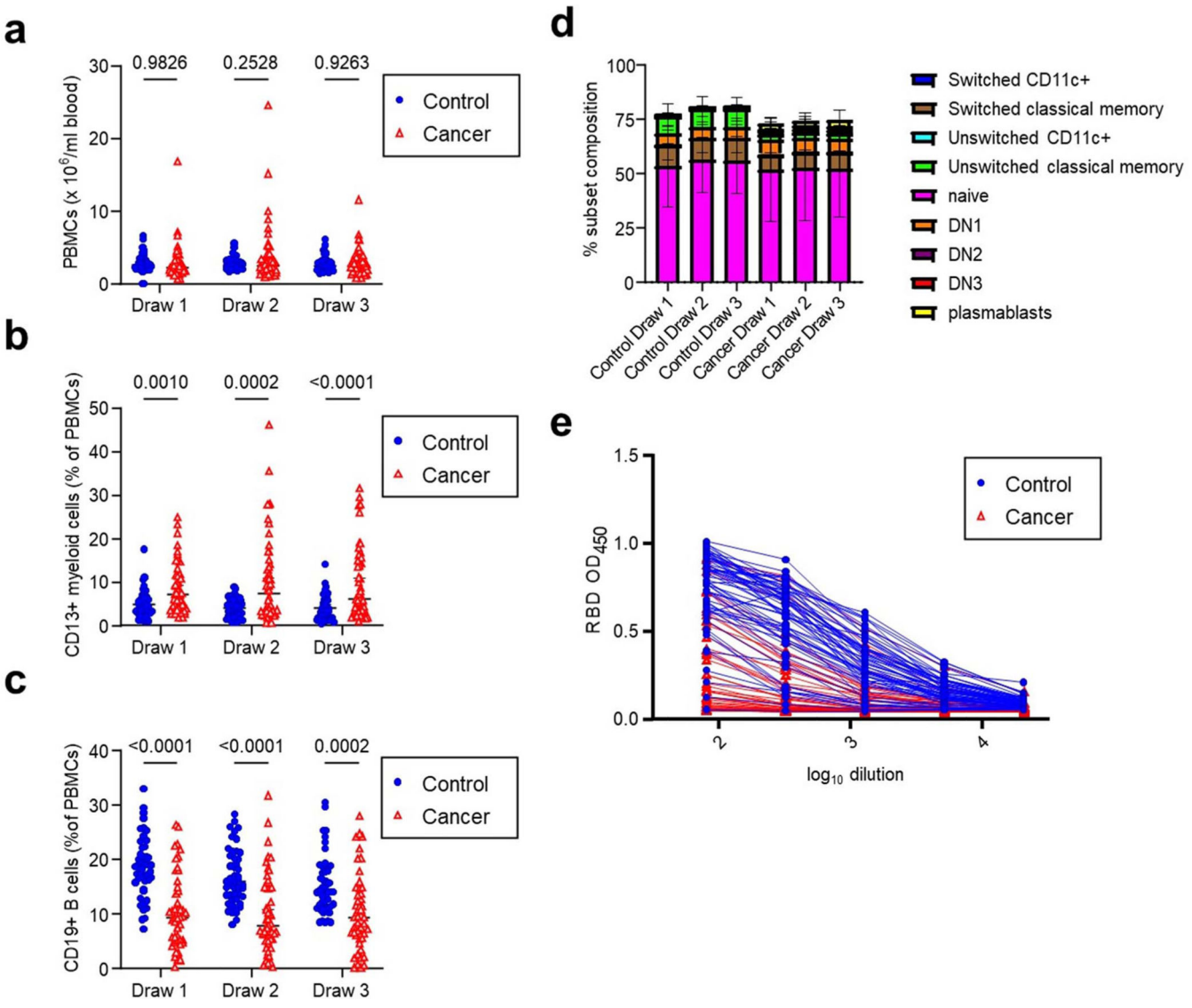

Extended Data Fig. 2. Cellular and serological characterization of blood samples from control and cancer cohorts.

a, PBMC frequencies of blood samples at each timepoint. Two-sided p-values from t-test statistics were calculated for pairwise differences using 2-way ANOVA. Post-hoc testing for multiple comparisons between draws was performed using Sidak's correction. Comparisons were made between cohorts matched for draw number. All data points represent biological replicates (n=50 for control cohort; n=53 for cancer cohort). b, CD19+ B cell frequencies of blood samples at each timepoint. Two-sided p-values from t-test statistics were calculated for pairwise differences using 2-way ANOVA. Post-hoc testing for multiple comparisons between draws was performed using Sidak's correction. Comparisons were made between cohorts matched for draw number. All data points represent biological replicates (n=50 for control cohort; n=53 for cancer cohort). c, CD13+ myeloid cell frequencies of blood samples at each blood draw. Two-sided p-values from t-test statistics were calculated for pairwise differences using 2-way ANOVA. Post-hoc testing for multiple comparisons between draws was performed using Sidak's correction. Comparisons were made between

cohorts matched for draw number. All data points represent biological replicates (n=50 for control cohort; n=53 for cancer cohort). d, B cell subset frequencies at each draw, descriptive statistics include mean ± SEM for n = 50 control and n = 53 cancer cohort participants for each subtype. e, Raw ELISA data for quantification of RBD titers shown in Figure 1d. A serum concentration beginning at 1:80 was serially diluted and area under the curve (AUC) values calculated. Lines connect the same individual at each dilution. Data from the third blood draw are shown for both the control and cancer cohort. Each individual curve represents a biological replicate (n=50 for control cohort; n=53 for cancer cohort).

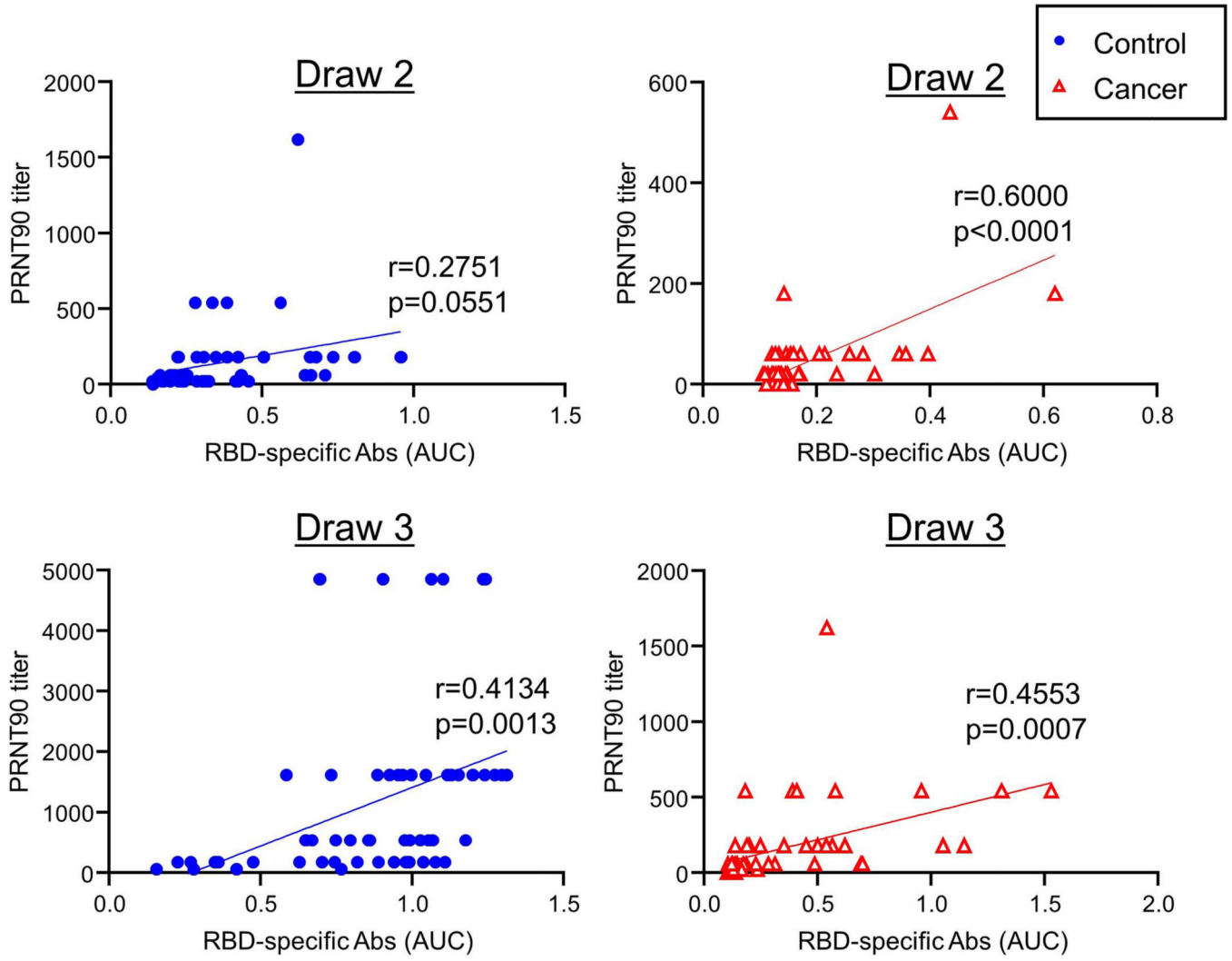

Extended Data Fig. 3. Correlation between RBD-binding antibodies and virus-neutralization.
RBD titers were plotted against PRNT levels for control and cancer cohorts at draws 2 and 3. Pearson correlation analyses were performed. All data points represent biological replicates (n=50 for control cohort; n=53 for cancer cohort).

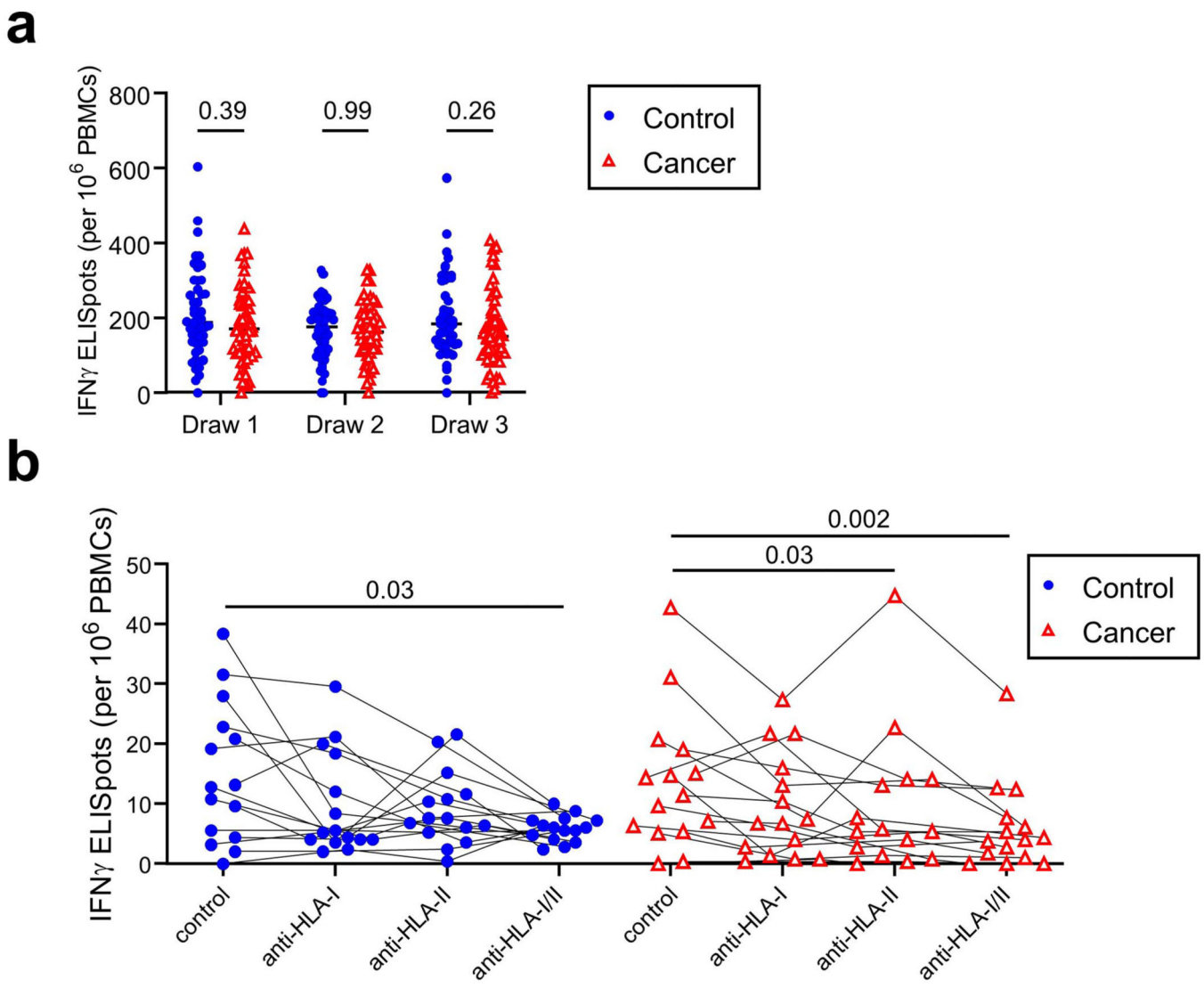

Extended Data Fig. 4. T cell activation in control and cancer cohorts.

a, PBMCs were cultured for 24 h in the presence of an activating anti-CD3 antibody. IFNγ-producing cells were quantified by ELISPOT. Two-sided p-values from t-test statistics were calculated for pairwise differences using 2-way ANOVA. Post-hoc testing for multiple comparisons between draws was performed using Sidak's correction. Comparisons were made between cohorts matched for draw number. All data points represent biological replicates (n=50 for control cohort; n=53 for cancer cohort). b, Spike-specific T cell activation was quantified in the presence or absence of anti-HLA-I and/or anti-HLA-II blocking antibodies. Two-sided p-values from t-test statistics were calculated using 1-way ANOVA. Post-hoc testing for multiple comparisons was performed using Tukey's correction. P-values >0.05 are not depicted. All data points represent biological replicates (n=15 for control cohort; n=16 for cancer cohort).

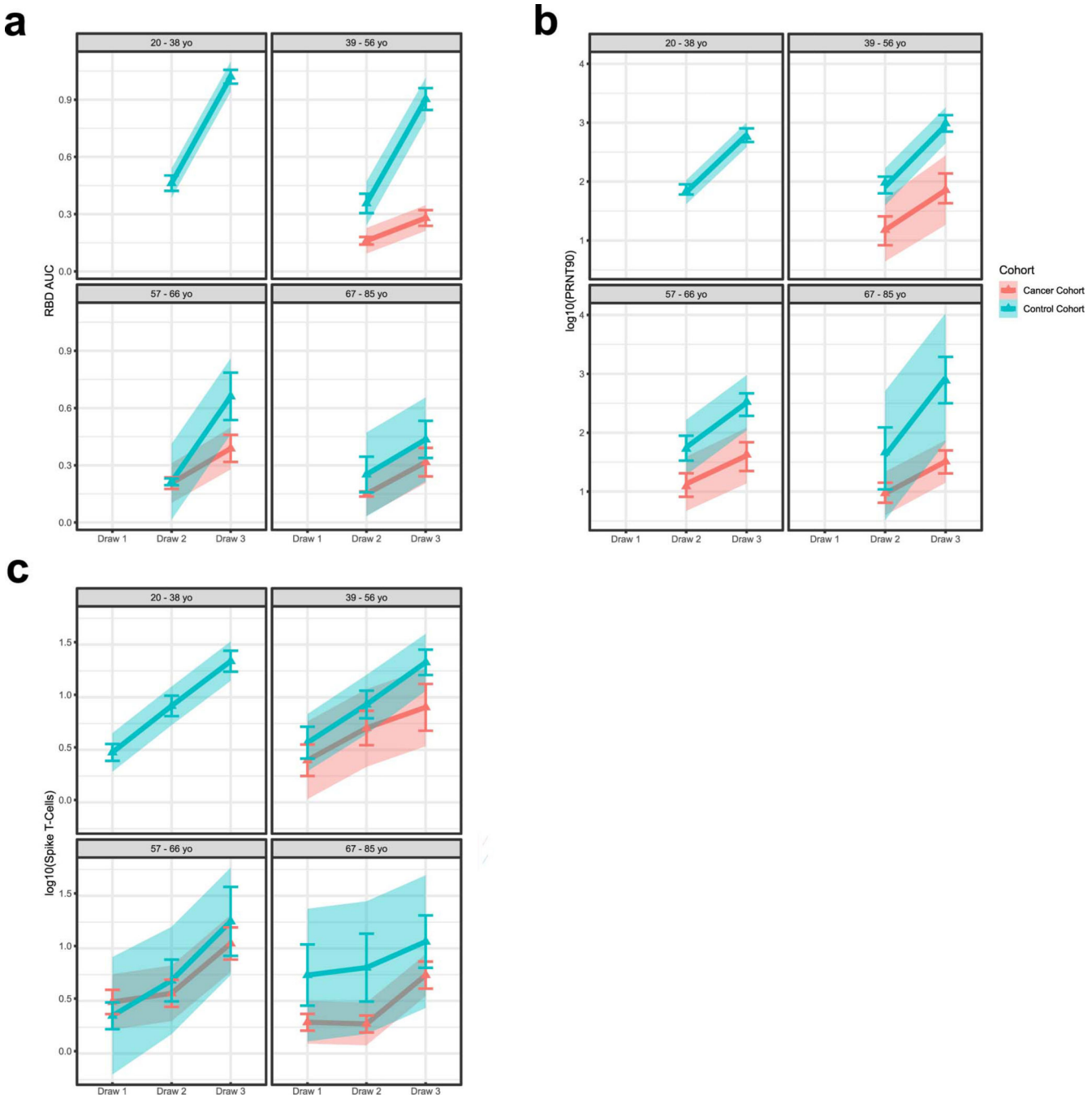

Extended Data Fig. 5. Age-moderated analysis of immunological parameters.

a, Trajectory between two draws for RBD AUC for each cohort stratified by age quartile. b, Trajectory between two draws for log10(PRNT90) for each cohort stratified by age quartile. c, Trajectory between three draws for Spike-specific T cell frequencies for each cohort stratified by age quartile. RBD AUC and cohort differences were moderated by age (p-value = 0.01). This effect was driven by the effect of age on the control cohort, increasing age was associated with lower RBD AUC, while the cancer cohort levels were similar across the three upper age quartiles. The difference between the cancer cohort and control cohort

was different at draw 3 for all age quartiles 2 – 4. Plots show the means and SEM for each draw along with the prediction intervals based on smoothing splines for each cohort There was no statistically significant difference in the relationship between log10(PRNT90) or Spike-specific T-cell frequencies by age. There was a degree of variability in Spike-specific T-cell frequency measurements in both cohorts though the trend in lower draw 3 measures in the cancer cohort remained consistent. The sample size for each age quartile was n = 0, 12, 20, 20 for the cancer cohort and n = 26, 14, 5, 5 for the control cohort.

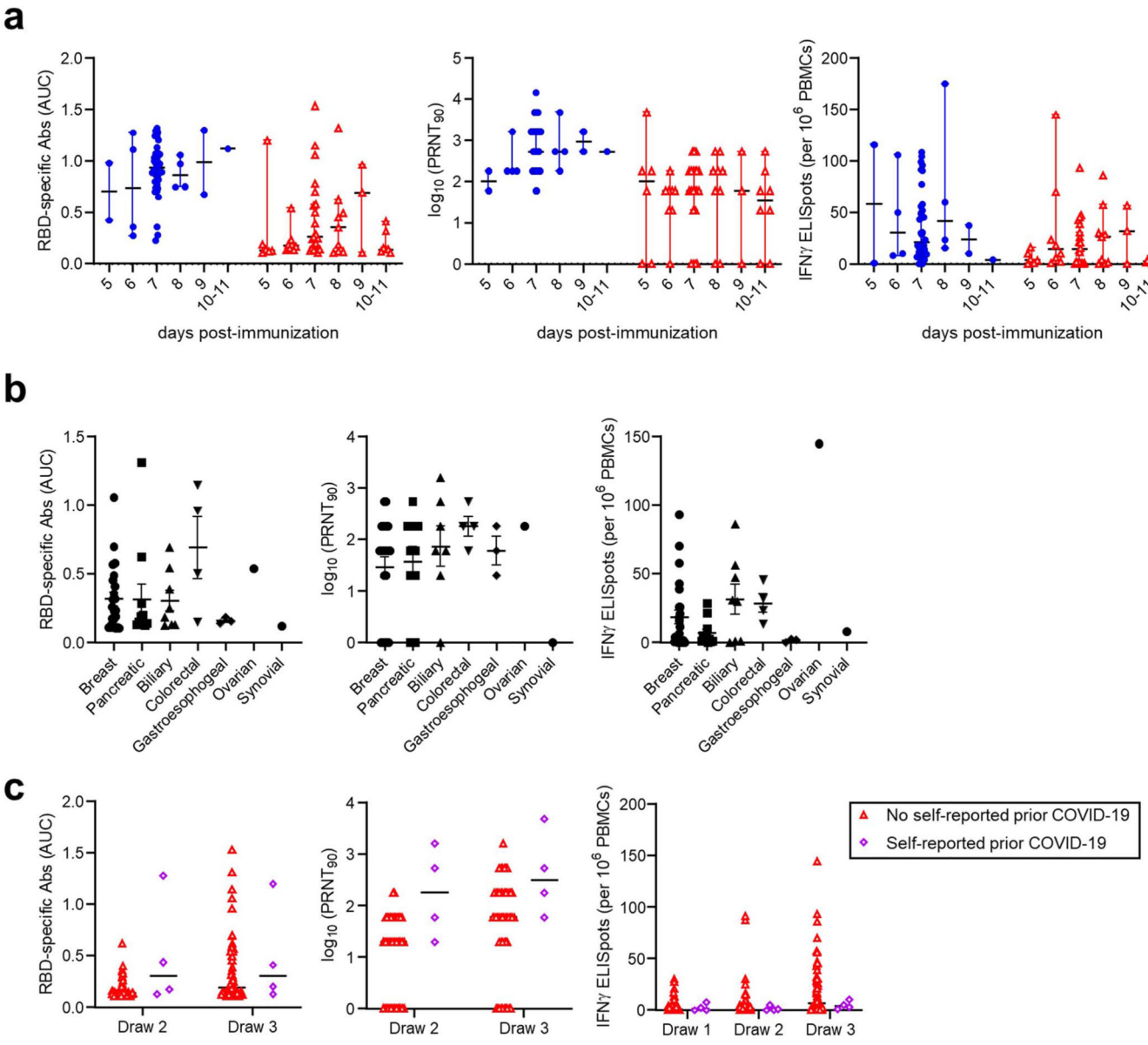

Extended Data Fig. 6. Immune responses grouped by time post-vaccination or tumor type.

a, RBD-specific antibodies, neutralizing titers, and Spike-specific T cells were plotted as a function of time after the second vaccination. Mean values + SEM are shown. Two-sided p-values from t-test statistics were calculated within each cohort using 1-way ANOVA with post-hoc Tukey's multiple comparisons test. No significant differences were observed. All

data points represent biological replicates (n=50 for control cohort; n=53 for cancer cohort). b, RBD-specific antibodies, neutralizing titers, and Spike-specific T cells were plotted as a function of tumor type. Mean values + SEM are shown. Two-sided p-values from t-test statistics were calculated using 1-way ANOVA with post-hoc Tukey's multiple comparisons test. No significant differences were observed. All data points represent biological replicates. c, RBD-specific antibodies, neutralizing titers, and Spike-specific T cells were plotted comparing participants who either did or did not self-report prior COVID-19. Mean values are shown. All data points represent biological replicates (breast: n=23; pancreatic cancer: n=11; biliary: n=8; colorectal: n=4; gastroesophogeal: n=3; ovarian: n=1; synovial: n=1).

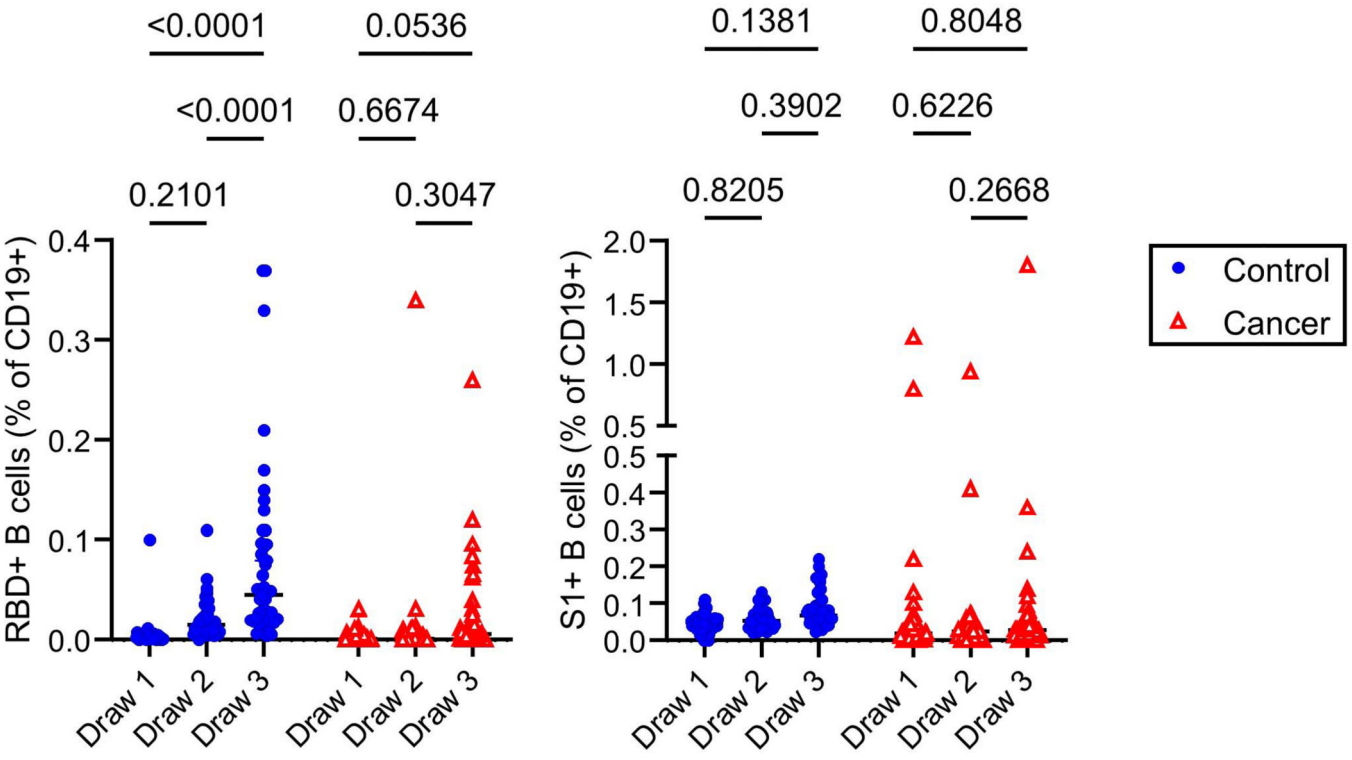

Extended Data Fig. 7. Quantification of RBD- and S1-specific B cells after vaccination.
RBD- and S1-specific CD19+ B cell frequencies were measured using gating strategies shown in Extended Data Figure 1 and Figure 4a. Cells that bind both RBD and S1 are annotated as RBD+, whereas cells that are specific only for S1 are denoted as S1+. Two-sided p-values from t-test statistics were calculated for pairwise differences using 2-way ANOVA. Post-hoc testing for multiple comparisons between draws was performed using Sidak's correction. Comparisons were made within cohorts. All data points represent biological replicates (n=50 for control cohort; n=53 for cancer cohort).

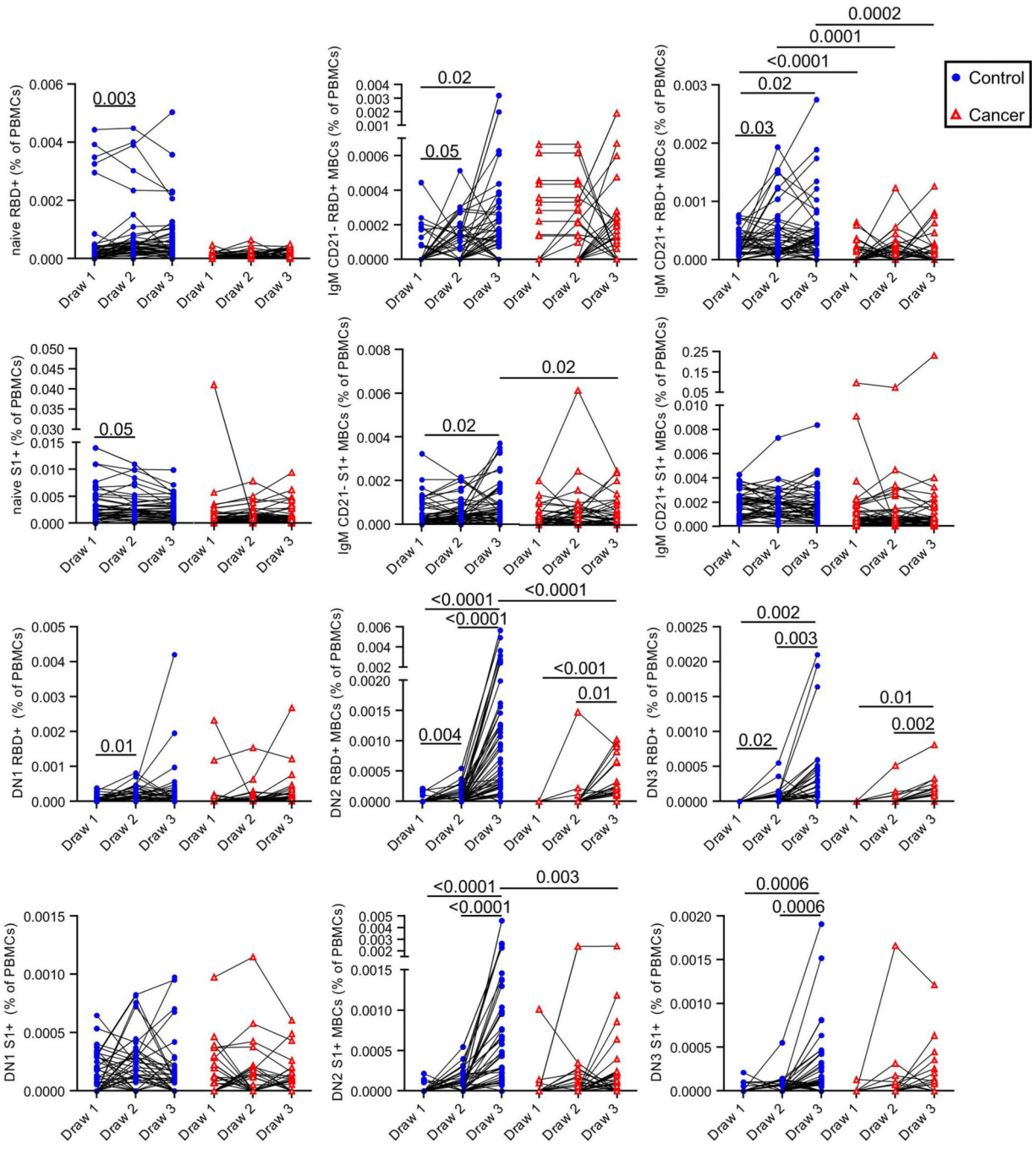

Extended Data Fig. 8. Quantification of memory B cell subsets after vaccination.

Cells that bind both RBD and S1 are annotated as RBD+, whereas cells that are specific only for S1 are denoted as S1+. Lines connect the same individual across blood draws, analyses were done on the arcsin of the square-root transformation, to standardize the small percentages. There is a statistically significant difference in slopes between cancer and control cohorts for DN2 RBD+ and S1+ ($p < 0.0001$ and < 0.0001, respectively) and the average rate of change is increasing in the control cohort for both DN2 RBD+ and S1+; with less dramatic slope increases with DN2 RBD+ and a flat trajectory for DN2 S2+

in the cancer cohort over time. Two-sided p-values from t-test statistics were calculated for pairwise differences using 2-way ANOVA. Post-hoc testing for multiple comparisons between draws was performed using Sidak's correction. Comparisons were made within cohorts or between cohorts by draw, p-values >0.05 are not depicted. All data points represent biological replicates (n=50 for control cohort; n=53 for cancer cohort).

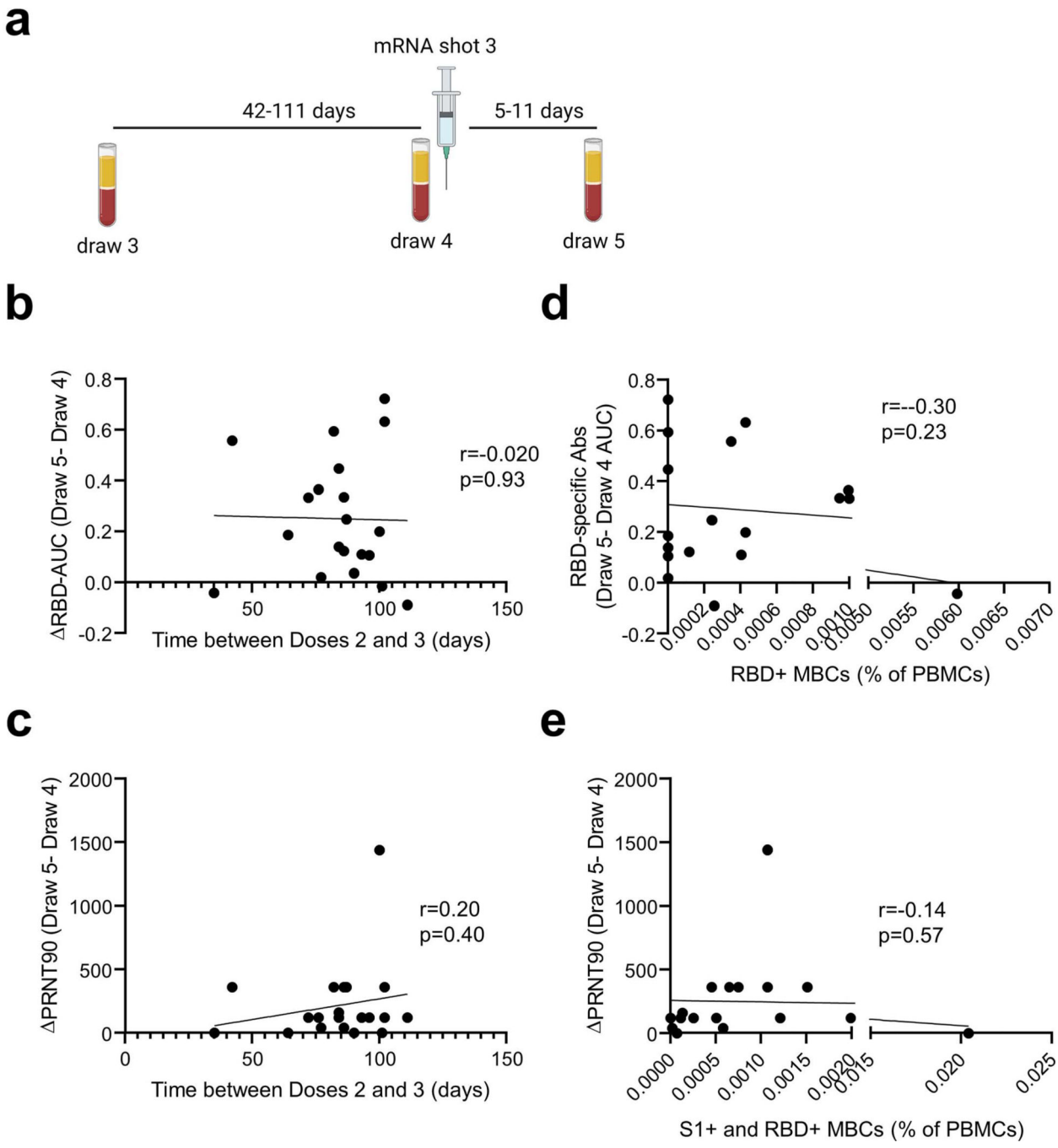

Extended Data Fig. 9. Correlation between memory B cells and anamnestic antibody responses.

a, RBD-specific memory B cell frequencies at Draw 3 (calculated as in Figure 4) were plotted against the difference in RBD antibody titers between Draws 4 and 5. Pearson's correlation analysis was performed. All data points represent biological replicates (n=20). b, RBD- and S1-specific memory B cell frequencies at Draw 3 (calculated as in Figure 4) were plotted against the difference in PRNT-90 titers between Draws 4 and 5. Pearson's correlation analysis was performed. All data points represent biological replicates (n=20).

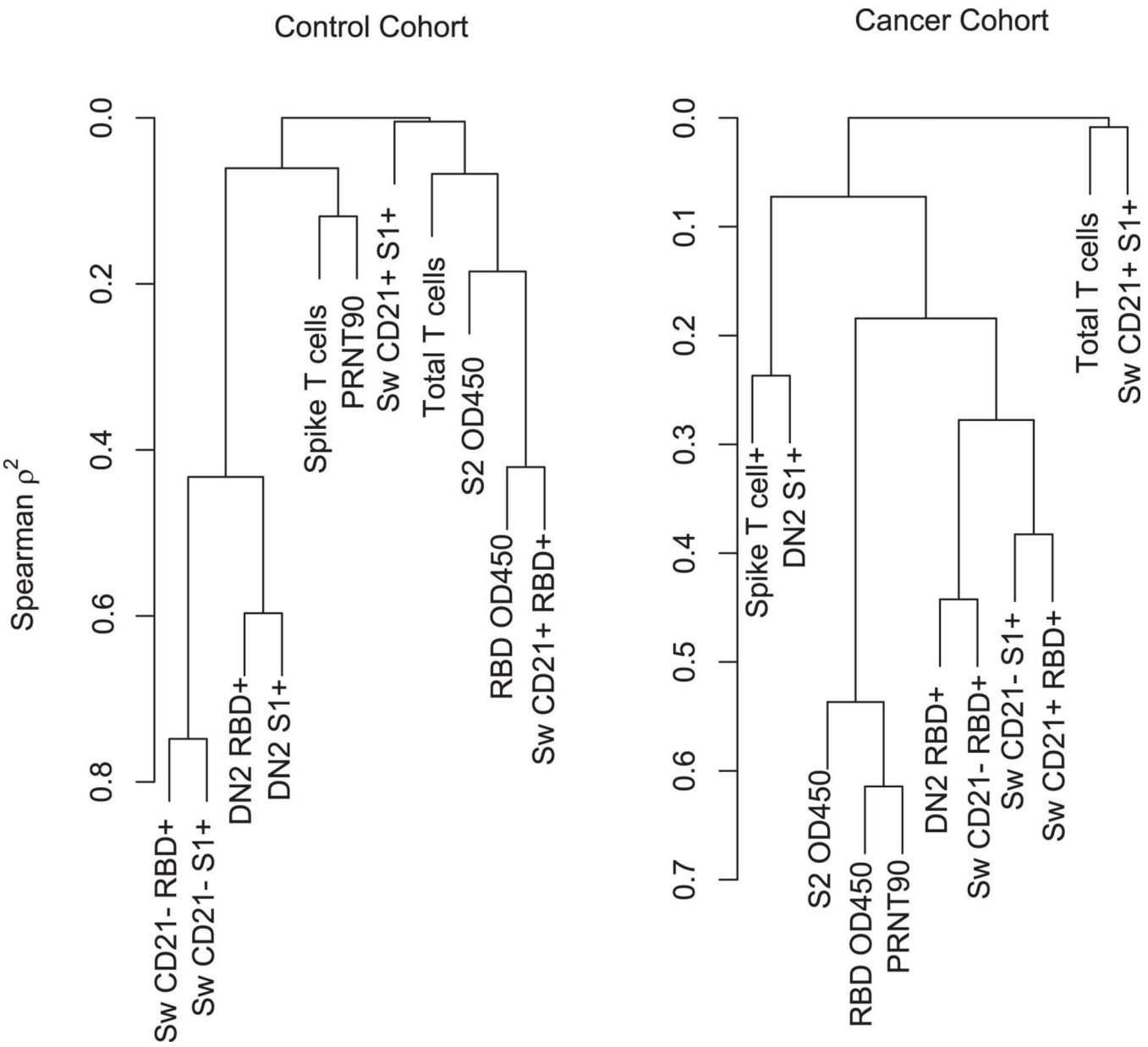

Extended Data Fig. 10. Hierarchical clustering of immunological parameters.

Hierarchical clustering at the variable level, using Spearman's rank order statistic was performed to evaluate both the correlation (similarity) of immune biomarkers after they are grouped into similar clusters. Of note is the different pattern of both clustering and similarity of the clustered variables between the control and cancer cohorts. Specifically, in the control

cohort the B-cell data group into two clusters (including both switched CD21+ and DN2) with a high degree of correlation (spearman correlation of 0.80) a pattern that was not seen in the cancer cohort, within which the only obvious cluster was that of the neutralizing titers, RBD and S2 OD -- with a correlation of 0.6.

Supplementary Material

Refer to Web version on PubMed Central for supplementary material.

Acknowledgements:

This work was supported by National Institutes of Health grants R01AI099108 and R01AI129945 (D.B.), R37AG020719 (J.N.Z.), T32AG058503 (T.J.R.) and from University of Arizona funds (D.B. and R.S.). We thank Marion Pepper (University of Washington) and Jason Netland (University of Washington) for technical assistance with tetramer stains. The funders had no role in study design, data collection and analysis, decision to publish or preparation of the manuscript. Schema in Figures 1A and Extended Data Figure 9a were created using Biorender.

Sana Biotechnology has licensed intellectual property of D.B. and Washington University in St. Louis. D.B. is a co-founder of Clade Therapeutics. B.J.L. has a financial interest in Cofactor Genomics, Inc. and Iron Horse Dx. P.C. receives research funding from Pfizer, BioAtla, Zentalis, Genentech, Eli-Lilly, Phoenix Molecular Designs, Amgen, Radius Pharmaceuticals, Carrick Therapeutics, and Angiochem and served on advisory boards for Novartis, Eli Lilly, Zentalis, Astra-Zeneca, Amgen, Bayer, Asthenex, Prosigna, Heron, Puma Biotechnology and Oncosec. R.T.S. receives research funding from Merck, Rafael Pharmaceuticals, ImmunoVaccine, Bayer, SeaGen, Exelixis, Pieris, LOXO Oncology, Novocure, NuCana, QED and has served as a consultant/advisor to Merck, Servier, Astra-Zeneca, EMD Serono, Taiho, QED, Incyte, Genentech, Basilea.

References:

1. Wu F et al. A new coronavirus associated with human respiratory disease in China. Nature 579, 265–269 (2020). [PubMed: 32015508]
2. Zhou P et al. A pneumonia outbreak associated with a new coronavirus of probable bat origin. Nature 579, 270–273 (2020). [PubMed: 32015507]
3. Polack FP et al. Safety and Efficacy of the BNT162b2 mRNA Covid-19 Vaccine. New England Journal of Medicine **0**, null (2020).**0**
4. Baden LR et al. Efficacy and Safety of the mRNA-1273 SARS-CoV-2 Vaccine. New England Journal of Medicine 384, 403–416 (2021).
5. Kuderer NM et al. Clinical impact of COVID-19 on patients with cancer (CCC19): a cohort study. Lancet 395, 1907–1918 (2020). [PubMed: 32473681]
6. Herishanu Y et al. Efficacy of the BNT162b2 mRNA COVID-19 vaccine in patients with chronic lymphocytic leukemia. Blood 137, 3165–3173 (2021). [PubMed: 33861303]
7. Deepak P et al. Effect of Immunosuppression on the Immunogenicity of mRNA Vaccines to SARS-CoV-2. Ann Intern Med (2021) doi:10.7326/M21-1757.
8. Boyarsky BJ et al. Antibody Response to 2-Dose SARS-CoV-2 mRNA Vaccine Series in Solid Organ Transplant Recipients. JAMA (2021) doi:10.1001/jama.2021.7489.
9. Monin L et al. Safety and immunogenicity of one versus two doses of the COVID-19 vaccine BNT162b2 for patients with cancer: interim analysis of a prospective observational study. The Lancet Oncology S1470204521002138 (2021) doi:10.1016/S1470-2045(21)00213-8.
10. Boyarsky BJ et al. Immunogenicity of a Single Dose of SARS-CoV-2 Messenger RNA Vaccine in Solid Organ Transplant Recipients. JAMA 325, 1784–1786 (2021). [PubMed: 33720292]
11. Ripperger TJ et al. Orthogonal SARS-CoV-2 Serological Assays Enable Surveillance of Low-Prevalence Communities and Reveal Durable Humoral Immunity. Immunity 53, 925–933.e4 (2020). [PubMed: 33129373]
12. Ladner JT et al. Epitope-resolved profiling of the SARS-CoV-2 antibody response identifies cross-reactivity with endemic human coronaviruses. Cell Rep Med 2, 100189 (2021).

13. Anderson EM et al. Seasonal human coronavirus antibodies are boosted upon SARS-CoV-2 infection but not associated with protection. Cell 184, 1858–1864.e10 (2021).
14. Nguyen-Contant P et al. S Protein-Reactive IgG and Memory B Cell Production after Human SARS-CoV-2 Infection Includes Broad Reactivity to the S2 Subunit. mBio 11, (2020).
15. Shrock E et al. Viral epitope profiling of COVID-19 patients reveals cross-reactivity and correlates of severity. Science 370, (2020).
16. Ng KW et al. Preexisting and de novo humoral immunity to SARS-CoV-2 in humans. Science 370, 1339–1343 (2020). [PubMed: 33159009]
17. Song G et al. Cross-reactive serum and memory B-cell responses to spike protein in SARS-CoV-2 and endemic coronavirus infection. Nat Commun 12, 2938 (2021). [PubMed: 34011939]
18. Hurlburt NK et al. Structural definition of a pan-sarbecovirus neutralizing epitope on the spike S2 subunit. 2021.08.02.454829 10.1101/2021.08.02.454829v1 (2021) doi:10.1101/2021.08.02.454829.
19. Greaney AJ et al. Antibodies elicited by mRNA-1273 vaccination bind more broadly to the receptor binding domain than do those from SARS-CoV-2 infection. Science Translational Medicine 13, eabi9915 (2021).
20. Piccoli L et al. Mapping Neutralizing and Immunodominant Sites on the SARS-CoV-2 Spike Receptor-Binding Domain by Structure-Guided High-Resolution Serology. Cell 183, 1024–1042.e21 (2020).
21. Sekine T et al. Robust T Cell Immunity in Convalescent Individuals with Asymptomatic or Mild COVID-19. Cell 183, 158–168.e14 (2020).
22. Rydyznski Moderbacher C et al. Antigen-Specific Adaptive Immunity to SARS-CoV-2 in Acute COVID-19 and Associations with Age and Disease Severity. Cell 183, 996–1012.e19 (2020).
23. Ogbe A et al. T cell assays differentiate clinical and subclinical SARS-CoV-2 infections from cross-reactive antiviral responses. Nature Communications 12, 2055 (2021).
24. McMahan K et al. Correlates of protection against SARS-CoV-2 in rhesus macaques. Nature 590, 630–634 (2021). [PubMed: 33276369]
25. Reynolds CJ et al. Discordant neutralizing antibody and T cell responses in asymptomatic and mild SARS-CoV-2 infection. Science Immunology 5, (2020).
26. Anderson EJ et al. Safety and Immunogenicity of SARS-CoV-2 mRNA-1273 Vaccine in Older Adults. New England Journal of Medicine 383, 2427–2438 (2020).
27. Goel RR et al. Distinct antibody and memory B cell responses in SARS-CoV-2 naïve and recovered individuals following mRNA vaccination. Science Immunology 6, (2021).
28. McCallum M et al. N-terminal domain antigenic mapping reveals a site of vulnerability for SARS-CoV-2. Cell 184, 2332–2347.e16 (2021).
29. Cerutti G et al. Potent SARS-CoV-2 neutralizing antibodies directed against spike N-terminal domain target a single supersite. Cell Host Microbe 29, 819–833.e7 (2021). [PubMed: 33789084]
30. Dogan I et al. Multiple layers of B cell memory with different effector functions. Nature Immunology 10, 1292–1299 (2009). [PubMed: 19855380]
31. Pape KA, Taylor JJ, Maul RW, Gearhart PJ & Jenkins MK Different B cell populations mediate early and late memory during an endogenous immune response. Science 331, 1203–7 (2011). [PubMed: 21310965]
32. Zuccarino-Catania GV et al. CD80 and PD-L2 define functionally distinct memory B cell subsets that are independent of antibody isotype. Nature Immunology 15, 631–637 (2014). [PubMed: 24880458]
33. Seifert M et al. Functional capacities of human IgM memory B cells in early inflammatory responses and secondary germinal center reactions. PNAS 112, E546–E555 (2015). [PubMed: 25624468]
34. Turner JS et al. Human germinal centres engage memory and naive B cells after influenza vaccination. Nature 586, 127–132 (2020). [PubMed: 32866963]
35. Lau D et al. Low CD21 expression defines a population of recent germinal center graduates primed for plasma cell differentiation. Science Immunology 2, eaai8153 (2017).

36. Wong R et al. Affinity-Restricted Memory B Cells Dominate Recall Responses to Heterologous Flaviviruses. Immunity 53, 1078–1094.e7 (2020).
37. Jenks SA et al. Distinct Effector B Cells Induced by Unregulated Toll-like Receptor 7 Contribute to Pathogenic Responses in Systemic Lupus Erythematosus. Immunity (2018) doi:10.1016/j.immuni.2018.08.015.
38. Knox JJ et al. T-bet+ B cells are induced by human viral infections and dominate the HIV gp140 response. JCI Insight 2,.
39. Woodruff MC et al. Extrafollicular B cell responses correlate with neutralizing antibodies and morbidity in COVID-19. Nat Immunol 21, 1506–1516 (2020). [PubMed: 33028979]
40. Kyu SY et al. Frequencies of human influenza-specific antibody secreting cells or plasmablasts post vaccination from fresh and frozen peripheral blood mononuclear cells. J Immunol Methods 340, 42–47 (2009). [PubMed: 18996127]
41. Amanna IJ Duration of Humoral Immunity to Common Viral and Vaccine Antigens. The New England Journal of Medicine 357, 1903–1915 (2007). [PubMed: 17989383]
42. Lavinder JJ et al. Identification and characterization of the constituent human serum antibodies elicited by vaccination. Proceedings of the National Academy of Sciences of the United States of America (2014) doi:10.1073/pnas.1317793111.
43. Purtha WE, Tedder TF, Johnson S, Bhattacharya D & Diamond MS Memory B cells, but not long-lived plasma cells, possess antigen specificities for viral escape mutants. J Exp Med 208, 2599–2606 (2011). [PubMed: 22162833]
44. Smith KGC, Light A, Nossal GJV & Tarlinton DM The extent of affinity maturation differs between the memory and antibody-forming cell compartments in the primary immune response. The EMBO Journal 16, 2996–3006 (1997). [PubMed: 9214617]
45. Angyal A et al. T-Cell and Antibody Responses to First BNT162b2 Vaccine Dose in Previously SARS-CoV-2-Infected and Infection-Naive UK Healthcare Workers: A Multicentre, Prospective, Observational Cohort Study. https://papers.ssrn.com/abstract=3820576 (2021) doi:10.2139/ssrn.3820576.
46. Wumkes ML et al. Serum antibody response to influenza virus vaccination during chemotherapy treatment in adult patients with solid tumours. Vaccine 31, 6177–6184 (2013). [PubMed: 24176495]
47. Puthillath A et al. Serological immune responses to influenza vaccine in patients with colorectal cancer. Cancer Chemother Pharmacol 67, 111–115 (2011). [PubMed: 20204362]
48. Abayasingam A et al. Long-term persistence of RBD+ memory B cells encoding neutralizing antibodies in SARS-CoV-2 infection. Cell Rep Med 2, 100228 (2021).
49. Mateus J et al. Selective and cross-reactive SARS-CoV-2 T cell epitopes in unexposed humans. Science 370, 89–94 (2020). [PubMed: 32753554]
50. Schulien I et al. Characterization of pre-existing and induced SARS-CoV-2-specific CD8+ T cells. Nat Med 27, 78–85 (2021). [PubMed: 33184509]
51. Grifoni A et al. Targets of T Cell Responses to SARS-CoV-2 Coronavirus in Humans with COVID-19 Disease and Unexposed Individuals. Cell 181, 1489–1501.e15 (2020).
52. Le Bert N et al. SARS-CoV-2-specific T cell immunity in cases of COVID-19 and SARS, and uninfected controls. Nature 584, 457–462 (2020). [PubMed: 32668444]
53. Weiskopf D et al. Phenotype and kinetics of SARS-CoV-2–specific T cells in COVID-19 patients with acute respiratory distress syndrome. Science Immunology 5, eabd2071 (2020).
54. Swadling L et al. Pre-existing polymerase-specific T cells expand in abortive seronegative SARS-CoV-2 infection. medRxiv 2021.06.26.21259239 (2021) doi:10.1101/2021.06.26.21259239.
55. Zhou D et al. Evidence of escape of SARS-CoV-2 variant B.1.351 from natural and vaccine-induced sera. Cell 184, 2348–2361.e6 (2021).
56. Edara V-V et al. Infection and Vaccine-Induced Neutralizing-Antibody Responses to the SARS-CoV-2 B.1.617 Variants. New England Journal of Medicine **0**, null (2021).**0**
57. Werbel WA et al. Safety and Immunogenicity of a Third Dose of SARS-CoV-2 Vaccine in Solid Organ Transplant Recipients: A Case Series. Ann Intern Med (2021) doi:10.7326/L21-0282.

58. Kamar N et al. Three Doses of an mRNA Covid-19 Vaccine in Solid-Organ Transplant Recipients. New England Journal of Medicine **0**, null (2021).**0**

59. Khoury DS et al. Neutralizing antibody levels are highly predictive of immune protection from symptomatic SARS-CoV-2 infection. Nature Medicine 1–7 (2021) doi:10.1038/s41591-021-01377-8.

60. Gilbert PB et al. Immune Correlates Analysis of the mRNA-1273 COVID-19 Vaccine Efficacy Trial. 2021.08.09.21261290 10.1101/2021.08.09.21261290v4 (2021) doi:10.1101/2021.08.09.21261290.

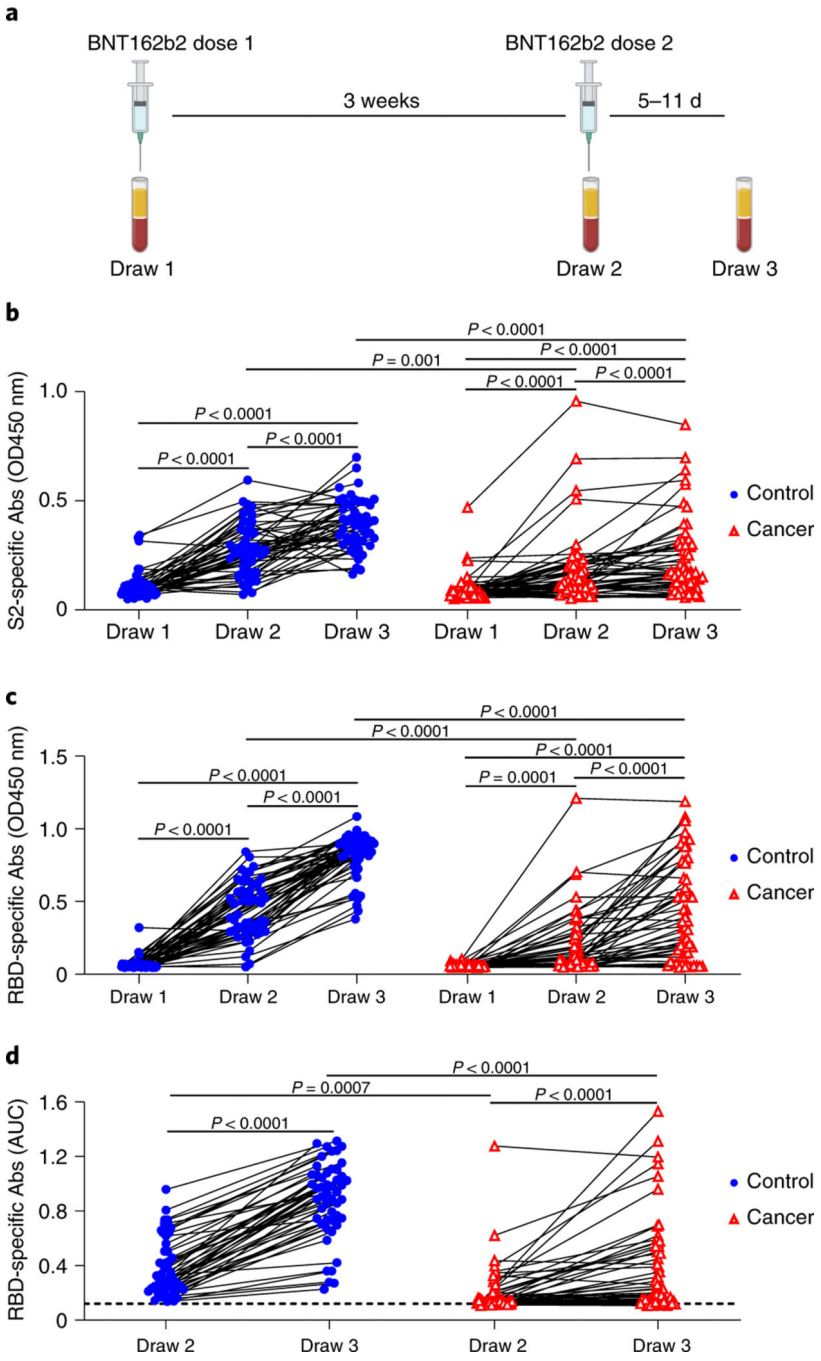

Figure 1: Antibody responses of cancer and control cohorts to mRNA vaccination.

a, Schematic of blood collection (draws) after vaccination. **b,** Semi-quantitative 1:40 serum dilution ELISA results for reactivity to the S2 region of SARS-CoV-2 Spike protein. Lines connect the same individual across timepoints. Repeated measures ANOVA examines the differences in slopes between cohorts, independently from the mean differences that were demonstrated at draw 3 between cohorts. There is a statistically significant difference in slopes between cancer and control cohorts ($p < 0.0001$) and the average rate of change is increasing at a steeper rate in the control cohort. These paired rates between draws by cohort

are statistically different in the control compared to the cancer cohort for both draws 1 and 2, though it is not different between draws 2–3 (p-values < 0.0001 and 0.2945, respectively). **c,** Semi-quantitative 1:40 serum dilution ELISA results for reactivity to the receptor binding domain (RBD) of SARS-CoV-2 spike protein. Lines connect the same individual at each draw. There is a statistically significant difference in slopes between cancer and control cohorts (p<0.0001) and the average rate of change is steeper in the control cohort. These paired rates between draws are statistically different in the control compared to the cancer cohort for both draw 1–2 and draw 2–3 (p-values<0.0001 and 0.0043, respectively). **d,** Quantitative titers of RBD antibodies in control and cancer cohorts. A serum concentration beginning at 1:80 was serially diluted 1:4 and area under the curve (AUC) values calculated. Lines connect the same individual across timepoints. There is a statistically significant difference between draws 2 and 3 between cancer and control cohorts (p< 0.0001) and the average rate of change is at a steeper increase in the control cohort. For **b-d**, two-sided p-values from t-test statistics were calculated for pairwise differences using 2-way ANOVA. Post-hoc testing for multiple comparisons between draws was performed using Sidak's correction. Comparisons were made either within cohorts or between cohorts at each draw, p-values >0.05 are not depicted. All data points represent biological replicates (n=50 for control cohort; n=53 for cancer cohort).

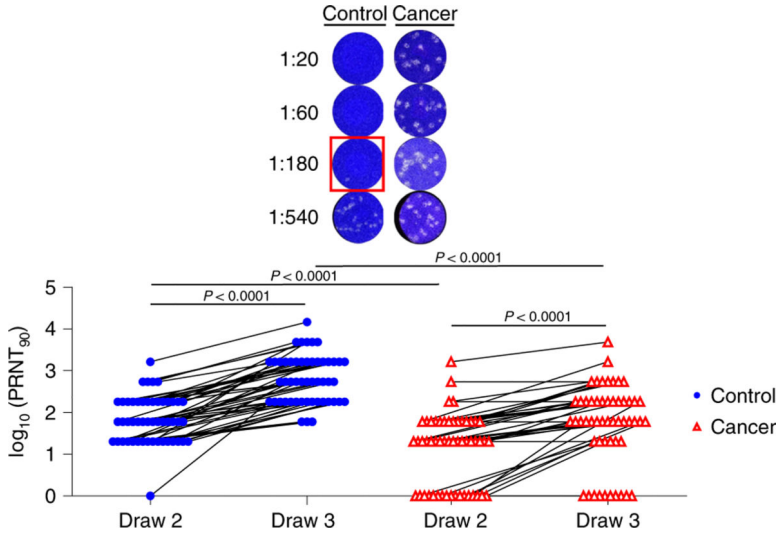

Figure 2: Neutralizing antibody responses of cancer and control cohorts to mRNA vaccination.

Virus neutralization assays were performed using the WA1 isolate of SARS-CoV-2. Serial 1:3 dilutions of serum were performed and tested for the ability to prevent plaques on Vero cells. The lowest concentration capable of preventing >90% of plaques was considered to be the PRNT90 value. Example images are shown for the control and cancer cohorts with the red box indicating the PRNT90 titer. Quantification is shown below. Lines connect the same individual across timepoints. There is a statistically significant difference between draw 2 and draw 3 between cancer and control cohorts ($p < 0.0001$) and the average rate of change is increasing at a steeper rate in the control cohort ($p = 0.0002$). Two-sided p-values from t-test statistics were calculated for pairwise differences using 2-way ANOVA. Post-hoc testing for multiple comparisons between draws was performed using Sidak's correction. Comparisons were made either within cohorts or between cohorts at each draw, p-values >0.05 are not depicted. All data points represent biological replicates (n=50 for control cohort; n=53 for cancer cohort).

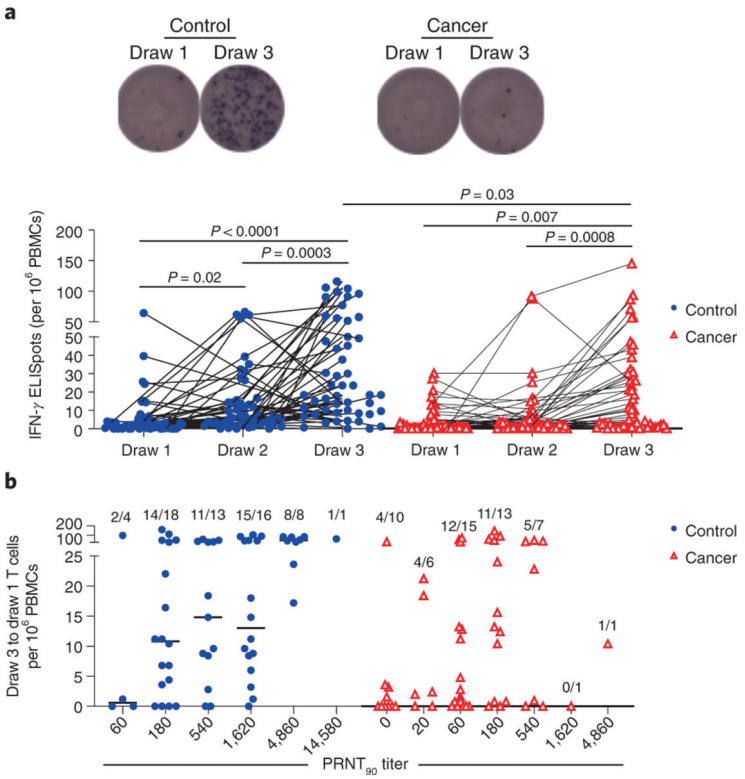

Figure 3: Spike-specific T cell responses of cancer and control cohorts to mRNA vaccination.

a, PBMCs were cultured for 24 h in the presence or absence of a pool of overlapping Spike protein peptides. IFNγ-producing cells were quantified by ELISPOT. Example images are shown for the control and cancer cohorts at timepoints 1 and 3. Quantification is shown below of the no peptide background-subtracted data. Lines connect the same individual across timepoints. There is a statistically significant difference in slopes between cancer and control cohorts (p = 0.0284) and the average rate of change is increasing steeper in the control cohort. While the overall rate of change was significant (draw 1 to draw 3, p = 0.0455), the rates of change between draw 1 to draw 2 and draw 2 to draw 3 were not statistically significant (p-values = 0.0642 and 0.9891, respectively). The inability to detect a statistical difference, particularly between draw 1 and draw 2, is likely due to sample size and variability as the cancer cohort difference is flatter than the cancer cohort between these two draws; these analyses were performed on a log-transformed scale. Two-sided p-values from t-test statistics were calculated for pairwise differences using 2-way ANOVA. Post-hoc testing for multiple comparisons between draws was performed using Sidak's correction. Comparisons were made either within cohorts or between cohorts at each draw, p-values >0.05 are not depicted. All data points represent biological replicates (n=50 for control cohort; n=53 for cancer cohort). **b,** Draw 1 Spike-specific T cell frequencies were subtracted from draw 3 frequencies as calculated in **a** and plotted as a function of PRNT90 titers. Frequencies of individuals with detectable Spike-specific T cells are shown above each group. All data points represent biological replicates (n=53).

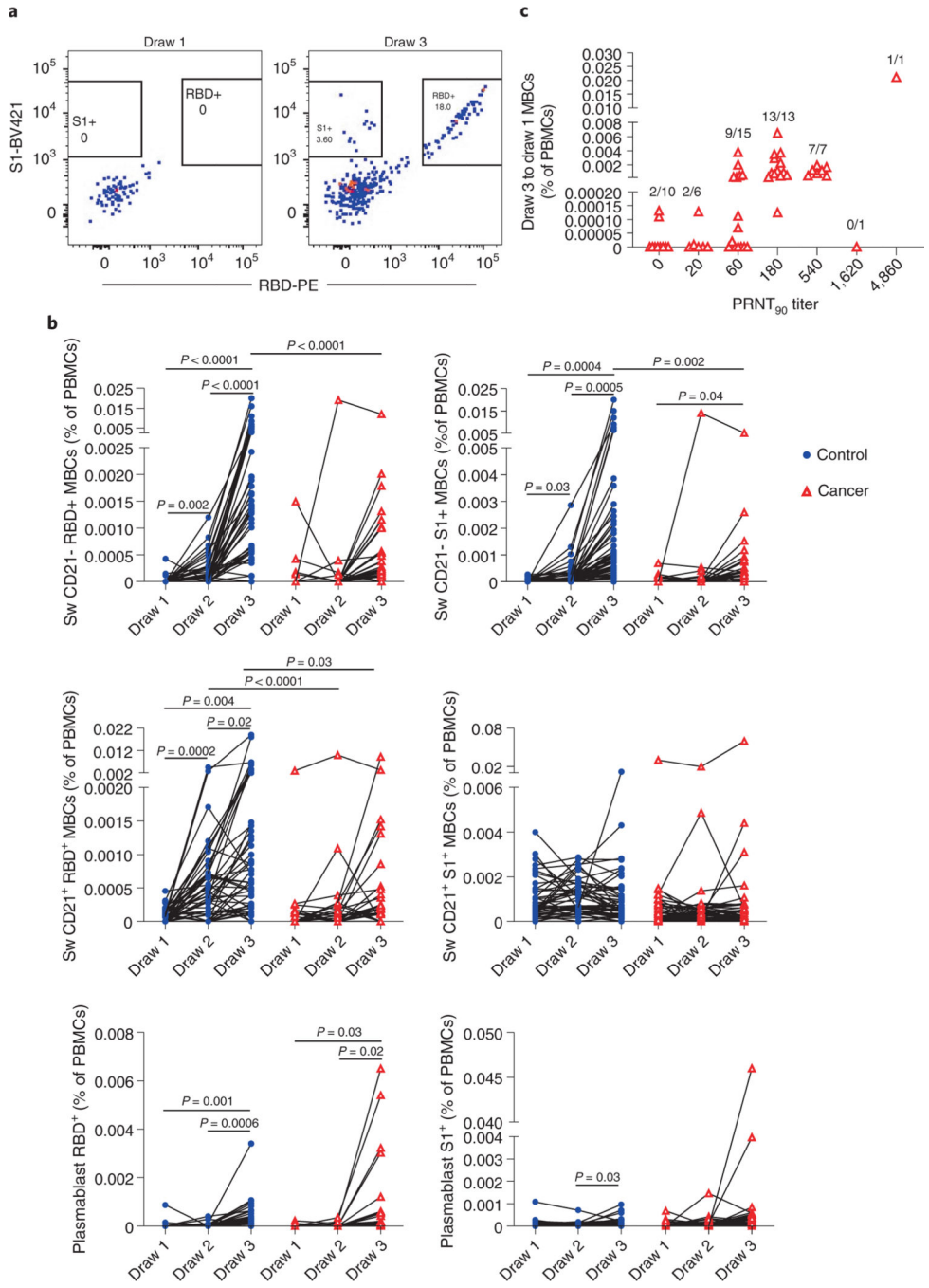

Figure 4: Memory B cell responses of cancer and control cohorts to mRNA vaccination.

a, Example gating strategy of RBD- and S1-specific CD21- isotype-switched memory B cells (full gating strategy is shown in Supplementary Figure). **b,** Quantification of memory B cell and plasmablast subsets after vaccination. Isotype-switched (Sw) memory B cells expressing or lacking CD21 are shown in plots along with plasmablasts. Cells that bind both RBD and S1 are annotated as RBD+, whereas cells that are specific only for S1 are denoted as S1+. Lines connect the same individual across blood draws, analyses were done on the arcsin of the square-root transformation, to standardize the small percentages. There is a

statistically significant difference in slopes between cancer and control cohorts for CD21- RBD+ and S1+ ($p < 0.0001$ and < 0.0001, respectively) and the average rate of change is increasing in the control cohort for both CD21- RBD+ and S1+ but the slope increases more dramatically between draw 2 and 3 in the control cohort compared to the cancer cohort with a modest linearly increasing slope. The average rate of change was statistically significantly different for CD21+ RBD+ ($p < 0.0001$), with an linearly increasing slope in the control cohort that is much steeper than the cancer cohort. There was no statistically significant difference in slopes between cancer and control cohorts for CD21+ S1+ ($p=0.1959$). Two-sided p-values from t-test statistics were calculated for pairwise differences using 2-way ANOVA. Post-hoc testing for multiple comparisons between draws was performed using Sidak's correction. Comparisons were made either within cohorts or between cohorts by draw, p-values >0.05 are not depicted. All data points represent biological replicates (n=50 for control cohort; n=53 for cancer cohort). **c,** RBD-specific DN2, DN3, and S1- and RBD-specific isotype-switched CD21- memory B cells were added for the cancer cohort. Summed draw 1 memory B cell frequencies were subtracted from the summation of draw 3 frequencies for each individual. These values were grouped by PRNT90 titers. Frequencies of individuals with detectable memory B cells are shown above each group. All data points represent biological replicates (n=53).

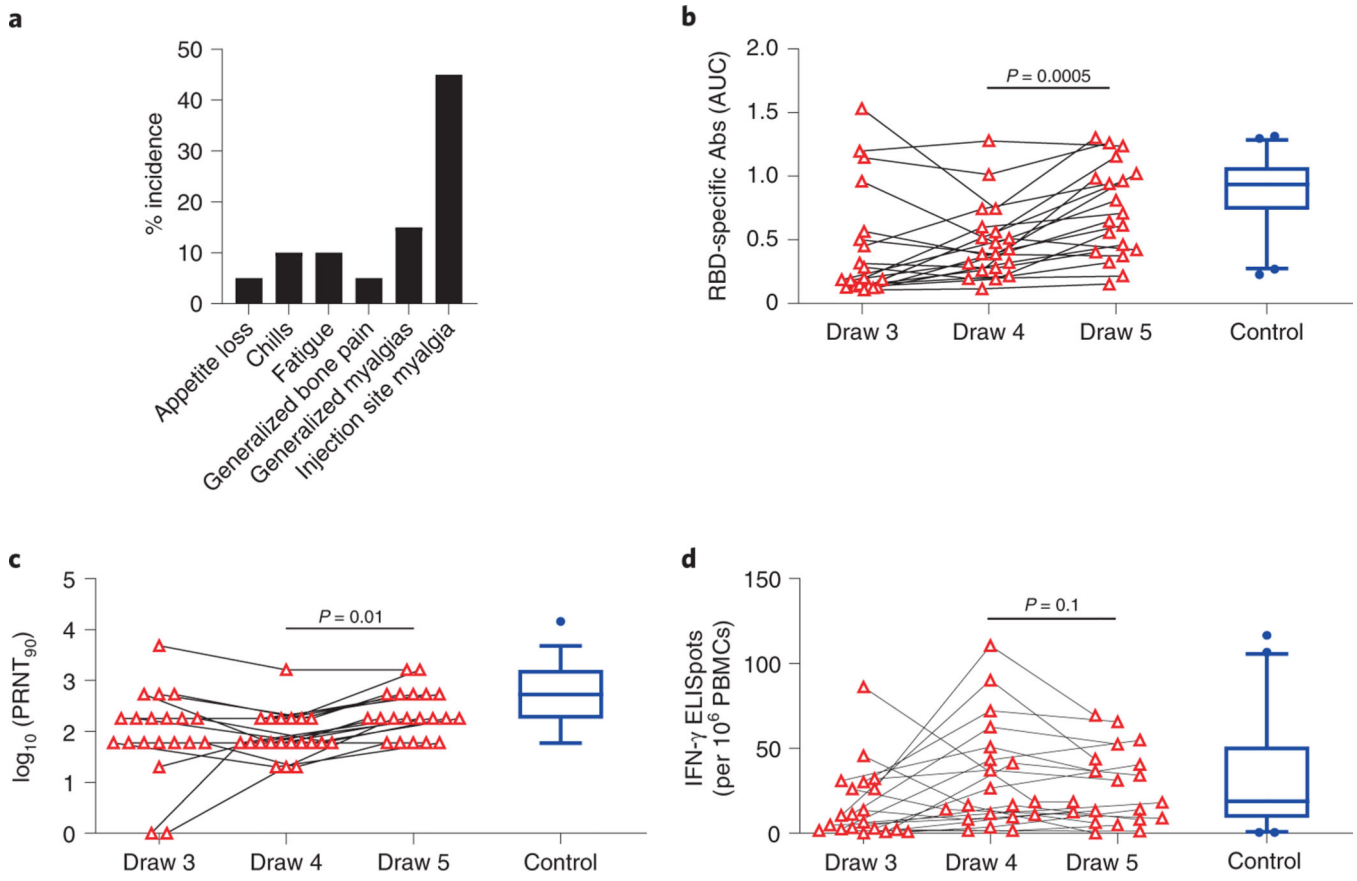

Figure 5: Antibody responses improve after a third immunization.

a, Frequencies of adverse events after third vaccine dose. **b**, RBD-specific antibody titers were quantified at the time of the 3rd immunization (draw 4) and 1 week afterwards (draw 5). Data from draw 3 are the same as those in Figure 1d and are shown again for context. Blue boxplot shows median and boundaries between the 1st and 3rd quartiles for the control cohort at draw 3; whiskers depict 5th-95th percentiles. All data points represent biological replicates (n=20). P-values are based on two-sided paired t-tests from the interventional (n = 20) cancer cohort based on draw 4 versus draw 5 comparisons; draw 3 cancer cohort (n=53) and control cohort (n=50) data are for descriptive comparison only. **c,** Neutralizing antibody titers were quantified at the time of the 3rd immunization (draw 4) and 1 week afterwards (draw 5). Data from draw 3 are the same as those in Figure 2. Blue boxplot shows median and boundaries between the 1st and 3rd quartiles for the control cohort at draw 3; whiskers depict 5th-95th percentiles. All data points represent biological replicates (n=20). P-values are based on two-sided paired t-tests from the interventional (n = 20) cancer cohort based on draw 4 versus draw 5 comparisons; draw 3 cancer cohort (n=53) and control cohort (n=50) data are for descriptive comparison only. **d,** Spike-specific T cell responses were quantified at the time of the 3rd immunization (draw 4) and 1 week afterwards (draw 5). Data from draw 3 are the same as those in Figure 3a. Blue boxplot shows median and boundaries between the 1st and 3rd quartiles for the control cohort at draw 3; whiskers depict 5th-95th percentiles. All data points represent biological replicates (n=20). P-values are based on two-sided paired t-tests from the interventional (n = 20) cancer cohort based on draw 4

versus draw 5 comparisons; draw 3 cancer cohort (n=53) and control cohort (n=50) data are for descriptive comparison only.

Table 1:

Characteristics of cohorts.

	Cancer Cohort (N=53)	Control Cohort (N=50)	Interventional Cohort (N=20)
Age			
Mean (SD)	63.7 (9.14)	41.3 (17.1)	63.1 (10.1)
Gender			
Female	42 (79.2%)	33 (66.0%)	15 (75.0%)
Male	11 (20.8%)	17 (34.0%)	5 (25.0%)
Prednisone			
Yes	1.00 (1.9%)	0 (0%)	0 (0%)
No	52.0 (98.1%)	50 (100%)	20(100%)
Recent Surgery			
Yes	2 (3.8%)	0 (0%)	1 (5.0%)
No	50 (96.2%)	50(100%)	19 (95.0%)
Other Vaccines			
Yes	0 (0%)	0 (0%)	0 (0%)
No	53 (100%)	50 (100%)	20 (100%)
Prior COVID Infection			
Yes	4 (5.8%)	1.00 (2.0%)	3 (15.0%)
No	49 (94.2%)	49 (98.0%)	17 (85.0%)
Radiation			
Yes	19 (35.8%)		7 (35.0%)
No	34 (64.2%)		13 (65.0%)
Missing	1 (1.9%)		0 (0%)
Days Since Treatment Prior to Draw 1			
Mean (SD)	16.3 (51.2)		5.05 (8.30)
Days Since Treatment Prior to Draw 2			
Mean (SD)	8.02 (7.64)		5.65 (5.71)
Days Since Treatment Prior to Draw 3			
Mean (SD)	15.8 (8.09)		7.35 (5.62)
Days Since Treatment Prior to Draw 4			
Mean (SD)			14.9 (18.6)
Tumor Type			
Gastroesophageal cancer	4 (7.5%)		
Pancreatic cancer	11 (20.8%)		8 (40.0%)
Biliary cancer	8 (15.1%)		3 (15.0%)
Colorectal cancer	4 (7.5%)		4 (20.0%)
Breast cancer	24 (45.3%)		5 (25.0%)
Sarcoma	1 (1.9%)		
Ovarian cancer	1 (1.9%)		

	Cancer Cohort (N=53)	Control Cohort (N=50)	Interventional Cohort (N=20)
Chemotherapy ¥			
Anthracycline-based	2 (4.0%)		0 (0%)
Fluoropyrimdine-based	14 (26.4%)		7 (35%)
Gemcitabine-based	13 (24.5%)		10 (50%)
Oral CDK4/6-based	10 (18.9%)		3 (15.0%)
Other Targeted Cytotoxics	4 (7.0%)		2 (10.0%)
Taxane/other antimicrotubule-based	9 (17.0%)		0 (0%)

¥ not mutually exclusive therefore don't sum to 100%

Interventional Cohort is a subset of the Cancer Cohort.